Article

Garnet as Indicator of Pegmatite Evolution: The Case Study of Pegmatites from the Oxford Pegmatite Field (Maine, USA)

Lorena Hernández-Filiberto [1,*], Encarnación Roda-Robles [2], William B. Simmons [3] and Karen L. Webber [3]

[1] Departamento de Ciencias de la Tierra y del Medio Ambiente, Universidad de Alicante, 03690 San Vicente del Raspeig, Spain

[2] Departamento de Geología, Universidad del País Vasco UPV/EHU, 48940 Leioa, Spain; encar.roda@ehu.es

[3] Maine Mineral & Gem Museum, P.O. Box 500, 99 Main Street, Bethel, ME 04217, USA; wsimmons@uno.edu (W.B.S.); kwebber@uno.edu (K.L.W.)

[*] Correspondence: lorehdezfiliberto@gmail.com

Abstract: Almandine-spessartine garnets, from the Oxford County pegmatites and the Palermo No. 1 pegmatite, record significant compositional variations according to the degree of evolution of their hosting rock. Garnets from the most fractionated pegmatites (Mt. Mica, Berry-Havey, and Emmons) show the highest Mn, Nb, Ta, Zr, and Hf values, followed by those from the intermediate grade pegmatites (Palermo No. 1) and, finally, garnets from the barren pegmatites show the lowest values (Perham and Stop-35). Iron, Ca, and Mg contents follow an inverse order, with the highest contents in the latter pegmatites. Major element zoning shows increasing Mn values from core to rim in most garnet samples, while trace element zoning is not systematic except for some crystals which show a core to rim depletion for most of these elements. Chondrite normalized HREE (Heavy Rare Earth Elements) spectra show positive slopes for garnets from barren pegmatites, both positive and negative slopes for those associated with the intermediate pegmatite, and negative or flat slopes in garnets from the highly fractionated pegmatites. Ion exchange mechanisms, including $Fe^{2+}_{-1}Mn^{2+}_{1}$, $(Fe^{2+}, Mn^{2+})_{-1}Si_{-1}Li_1P_1$; and, $(Y, Ho^{3+})_2(vac)_1(Fe^{2+}, Mn^{2+})_{-3}$, could explain most of the compositional variations observed in these garnets. These compositional variations are the reflection of the composition of the pegmatitic magma (barren pegmatites originate from a more ferromagnesian magma than fractionated pegmatites); and of the coexisting mineral phases competing with garnets to host certain chemical elements, such as biotite, schorl, plagioclase, apatite, Fe-Mn phosphates, Nb-Ta oxides, zircon, xenotime, and monazite.

Keywords: garnet; pegmatites; petrogenetic indicator; Oxford pegmatite field; Maine

1. Introduction

Garnet is a common accessory mineral in many granitic pegmatites [1]. The crystalline structure of this nesosilicate is formed by SiO_4 tetrahedra, divalent metal cations in the A position and trivalent cations in the B position. SiO_4 tetrahedra alternate with BO_6 octahedra, sharing vertices. This structure allows garnet to accommodate a wide variety of cations with different ionic radii and, as a consequence, garnet shows a great compositional variety [2]. The A position is often occupied by Ca, Fe^{2+}, Mg, or Mn^{2+}; whereas the B position host Al, Cr^{3+}, Fe^{3+}, Mn^{3+}, Si, Ti, V^{3+}, or Zr. The general formula $A_3B_2(SiO_4)_3$ defines the garnet supergroup [3]. Commonly, garnet composition corresponds to intermediate members between the various solid solutions. The garnet supergroup is quite extensive and complex. The most common species include pyrope ($Mg_3Al_2(SiO_4)_3$), almandine ($Fe_3Al_2(SiO_4)_3$), spessartine ($Mn_3Al_2(SiO_4)_3$), grossular ($Ca_3Al_2(SiO_4)_3$), andradite ($Ca_3Fe_2(SiO_4)_3$), and uvarovite ($Ca_3Cr_2(SiO_4)_3$) [4].

Despite garnets not forming in all pegmatites around the world, this nesosilicate is a common accessory phase in the pegmatites from the Oxford County (Maine, USA). As in other pegmatitic belts, when pegmatites are internally zoned, garnet occurs mainly in

their border, wall, and intermediate zones. In addition, in many pegmatites from this region, garnet constitutes a narrow strip, located below the core zone of the pegmatitic bodies, which is locally known as the 'garnet layer'. Since the beginning of the 20th century, the garnet layer has been used as a guide in the exploration of pegmatites from the Oxford field, especially Mt. Mica and Mt. Apatite, as this layer underlines the core zone of the pegmatites, where the mineralized pockets are commonly located [5]. Other characteristics associated with the garnet layer have also been used as pockets indicators, such as the texture and mineral association: e.g., the appearance of blackish to bluish tourmaline rims around garnet crystals for decades has been known to be indicative of pockets containing gemmy material [6]. Over the years, numerous descriptions have been made in the Oxford field about the mineralogy of both pegmatites and the garnet layer, e.g., [7–9]. The formation of the garnet layer has been recently interpreted as the product of the oscillatory nucleation and crystallization of a boundary layer [6,10].

Garnet composition has previously been used as an indicator in the exploration of diamonds and Pb-Zn deposits [11]. Over the years, some studies have also been developed on the compositional variations of garnets from different pegmatites around the world [1,11–17], giving interesting results. These variations may reflect the chemistry of pegmatitic magmas, the reactions between garnets and their associated minerals, as well as the pressure and temperature conditions during crystallization. As a consequence, garnets constitute important indicators of the fractionation degree of the pegmatites and of the extent of fractionation of the pegmatitic magmas. For example [12,17], observed that the most evolved pegmatites usually contain garnets of the spessartine variety. However, given the great compositional variability of minerals within a zoned pegmatitic body, valid comparisons may only be made by comparing garnets from the same unit of different pegmatites.

Since pegmatites from the Oxford field present a wide evolutionary range from barren bodies to highly evolved pegmatites, and they usually show a garnet layer, detailed chemical characterization of these garnets may be used to determine whether compositional variation could indicate the fractionation degree of their hosting pegmatite. In this study, garnets from highly evolved (Mt. Mica, Berry-Havey, and Emmons), intermediate (Palermo No. 1) and barren (Perham and Stop-35) pegmatites have been analyzed to determine if there are geochemical parameters capable of reflecting the fractionation degree of their hosting pegmatite.

2. Geological Setting

The studied pegmatites belong to the Oxford pegmatite field of Maine (USA), except for Palermo No.1 pegmatite, which is located at the Grafton pegmatite field of New Hampshire (USA) (Figure 1). Both pegmatite fields are located in the "Central Maine Belt" (CMB), a large synclinorium composed of Paleozoic metasediments [18] intruded by Ordovician to Mesozoic plutonic rocks [19] and trending NE–SW between New Brunswick (Canada) and Connecticut (USA) [20]. The CMB is the result of multiple orogenies associated with the Appalachian formation. Metamorphism and migmatitization are related to a major regional metamorphic event coupled with plutonism during the Acadian orogeny. Some authors (e.g., [21]) suggested that some of these plutonic intrusions were post-tectonic. Peak metamorphism is located at CMB's core [22] where the studied pegmatites are located, and include upper amphibolite facies with migmatites to the SW of the Oxford field, and green-schist facies to the NE [23,24].

Most pegmatites from the Oxford field occur within the "Sebago Migmatite-Granite Complex" (MGC) [25], which includes both the Sebago Pluton and the surrounding migmatites. The fractionation degree of the studied pegmatites ranges from barren bodies to highly evolved pegmatites showing well-developed internal zoning [9]. They intrude in every rock type of the MGC, either concordantly to the host rock foliation or as irregular and discordant bodies [26]. A garnet layer is commonly distinguished below the core zone of these pegmatites and commonly is accompanied by a tourmaline layer that occurs

next to it [26]. The origin of these pegmatites is still a matter of debate. [25] date the MSC in 376 Ma, while the age of the Sebago Pluton and other minor granitic rocks is 293 Ma. Other authors (e.g., [27]) dated the pegmatitic bodies between 250 and 270 Ma. This age difference between the Sebago Pluton and the pegmatites is in contrast to previous works (e.g., [20,28]), which suggested that these pegmatites were the product of fractional crystallization of the Sebago Pluton or pegmatitic leucogranites. Other authors (e.g., [29,30]) propose anatexis of the migmatites and metasedimentary host rocks as the origin for these pegmatites.
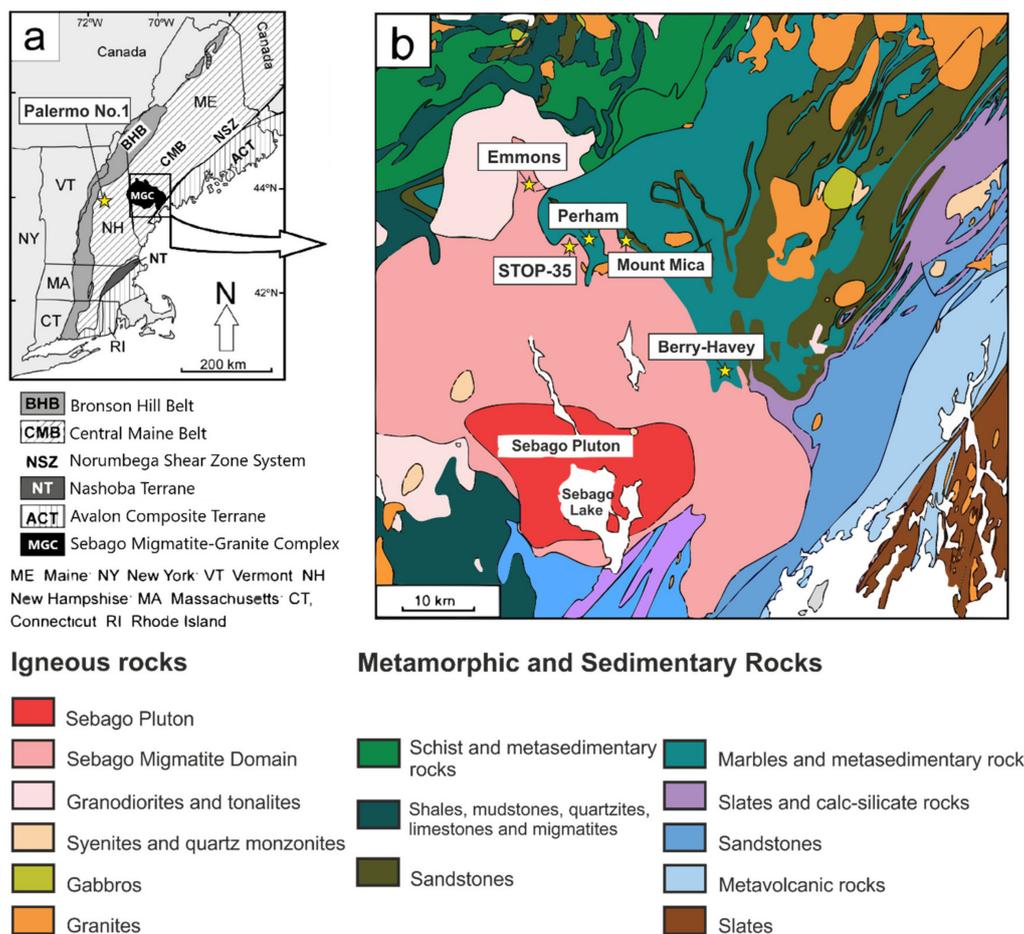

Figure 1. (**a**) Geographic location of the Oxford and Grafton pegmatite fields. Modified from [21]; (**b**) Lithological map of the Oxford pegmatite field modified from [20,31–33].

3. Sampling and Analytical Methods

Garnet samples were taken from the garnet layer of the Berry-Havey, Mt. Mica, and Emmons evolved pegmatites. As some of these pegmatites also present a tourmaline layer close to the garnet layer, garnet samples from Mt. Mica and Berry-Havey pegmatites were taken at different distances from the tourmaline layer. Garnets from the Palermo No. 1 pegmatite, with an intermediate fractionation degree, were taken from the innermost portions of their intermediate zone, which is the equivalent position to the garnet layer inside the evolved pegmatites. The barren Perham and Stop-35 pegmatites lack internal zoning. In these cases, garnet samples were taken from the intermediate parts of the bodies. In addition to the pegmatitic garnet, two garnet samples were taken from the migmatitic rocks hosting the Emmons and Stop-35 pegmatites for comparison.

A Cameca SX-100 electron microprobe (Gennevilliers, France) equipped with four wavelength-dispersive spectrometers from the University of Granada (Spain), was used to perform over 80 analyses of garnet's major elements. Both natural and synthetic standards

were used: fluorite (F), sanidine (K), synthetic $MnTiO_3$ (Mn, Ti), diopside (Ca), synthetic Fe_2O_3 (Fe), albite (Na), periclase (Mg), synthetic SiO_2 (Si), synthetic Cr_2O_3 (Cr), and synthetic Al_2O_3 (Al). Operating conditions were 20 kV accelerating voltage, 20 nA beam current, and a beam diameter of about 2 μm. Data were reduced using the procedure of [34]. Analytical errors are estimated to be on the order of ±1–2%.

Trace element analyses were performed using a LA-ICP-MS located at the "Centro de Instrumentación Científica" (CIC) at the University of Granada (Spain). Close to 100 analyses were made on representative garnet samples from the different pegmatites. All these analyses were performed on samples already analyzed by electron-microprobe for major and minor elements. These analyses were conducted with a 231 nm ESI NWR 213 laser (Elemental Scientific Lasers, MT, USA) coupled to a Perkin Elmer NexION 2000b ICP-MS (PerkinElmer, Ontario, Canada) with a shielded plasma torch, using the NIST-610 glass as standard. The ablation was carried out in a He atmosphere. The laser beam was fixed to a 95 mm wide square section and a 30 μm diameter. The spot was pre-ablated for 45 s using a laser repetition rate of 10 Hz and 40% output energy. Then the spot was ablated for 60 s at 10 Hz with a laser output energy of 75%. To keep the laser focused during ablation, the sample stage was set to move upward 5 mm every 20 s. A typical session of analysis of a single thin section began and ended with the analysis of the NIST-610 glass (about 450 ppb of each element), which was also analyzed every nine spots to correct for drift. Silicon was used as an internal standard. Data reduction was carried out with a custom software (freeware available from F. Bea) of the STATA commercial package (London, UK). This software permits identification and elimination of outliers, blank subtraction, drift correction, internal standard correction and conversion to concentration units. The precision, calculated on the five to seven replicates of the NIST-610 measured in every session, is in the range ±3% to ±7% for most elements. In conditions described, detection limits calculated by measuring five replicates of a large and homogeneous crystal of astrophyllite, ranged from better than 0.01 ppm for REE, Y, Th, and U, to about 0.5 ppm for Li.

4. Pegmatites Description

4.1. Mount Mica

The Mt. Mica pegmatite is a Li-rich pegmatite intruding concordantly into a biotite schist unit within the MGC, with a thickness that ranges 1–8 m down-dip along the dyke, strikes NE–SW, and dips about 20° SE [6]. The pegmatite shows an asymmetrical and poorly developed internal zoning, with a wall zone and an intermittent intermediate zone and the common presence of pockets with sizes ranging from a few cm^3 to 500 m^3 in the core zone. A garnet layer appears in the wall zone of the foot-wall (Figure 2), which can be double in some parts [29,35].

The wall zone is mainly composed of quartz, plagioclase, muscovite, and schorl; the intermediate zone consists of quartz and plagioclase, with minor tourmaline and muscovite; while the core consists of blocky quartz, albite, K-feldspar, and Li-rich tourmaline. Lepidolite pods are common in the core zone, where altered spodumene and montebrasite may also be present [6].

The garnet layer consists of a quartz, plagioclase and minor muscovite matrix containing abundant garnet and tourmaline crystals. According to [6], apatite and rare cookeite may also be present in this layer. The size of garnet crystals ranges from 0.5 to 5 cm in diameter, showing most commonly a euhedral habit and a reddish color (Figure 3a). Tourmaline rims often occur around the garnet crystals, especially in zones adjacent to pockets containing elbaite and other minerals typically associated with the most evolved parts of the pegmatite in the core zone. The tourmaline rims vary from a black color in the inner part, in direct contact with the garnet, to a bluish color in the outer part (Figure 3a). Some garnets also show a fine-grained muscovite rim (Figure 4a,b). Garnet crystals are usually crossed by numerous fractures (Figure 4a,b) some of which contain more evolved species such as pollucite [6].
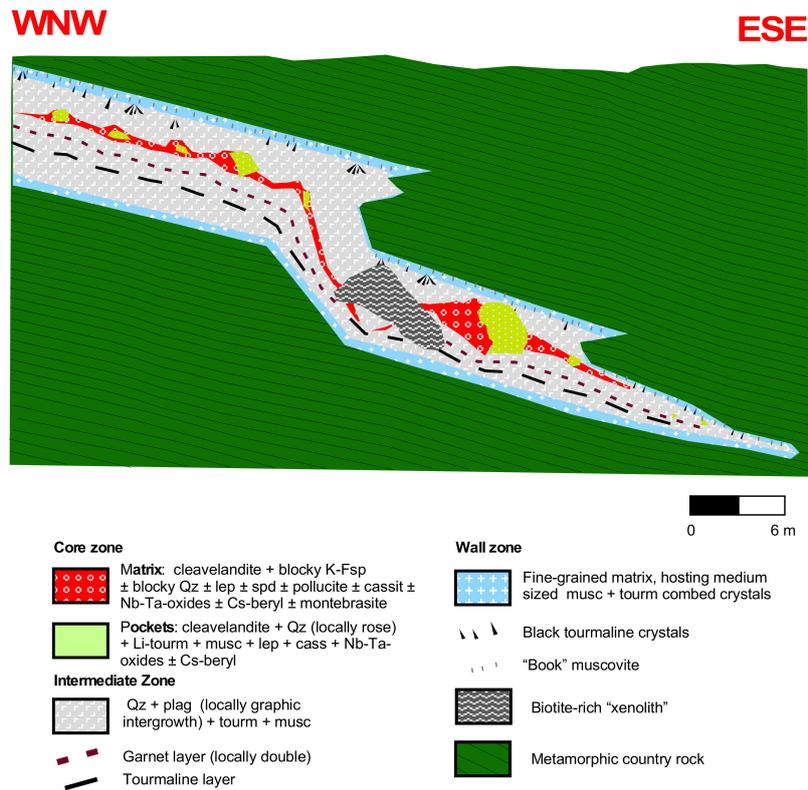
Figure 2. Idealized cross-section of the Mt. Mica pegmatite. Modified from Roda-Robles in [36].
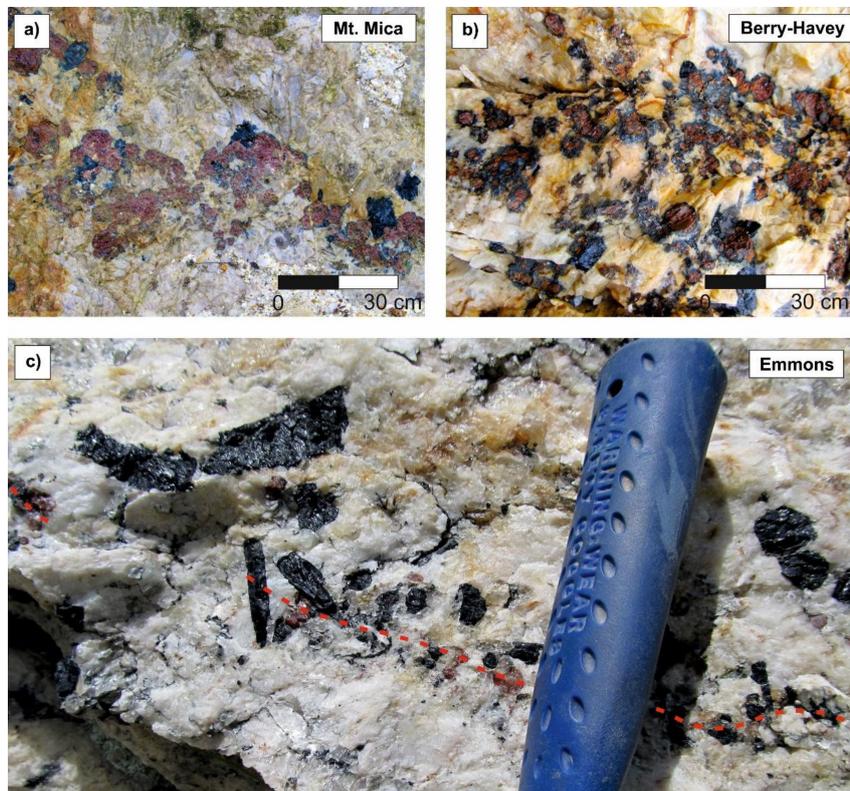

Figure 3. Garnet layer of three of the studied pegmatites from the Oxford field. Both Mt. Mica (**a**), and Berry-Havey (**b**), pegmatites show some garnets with tourmaline rims; (**c**) Garnet layer from the Emmons pegmatite (red dashed line) close to a schorl-rich level.
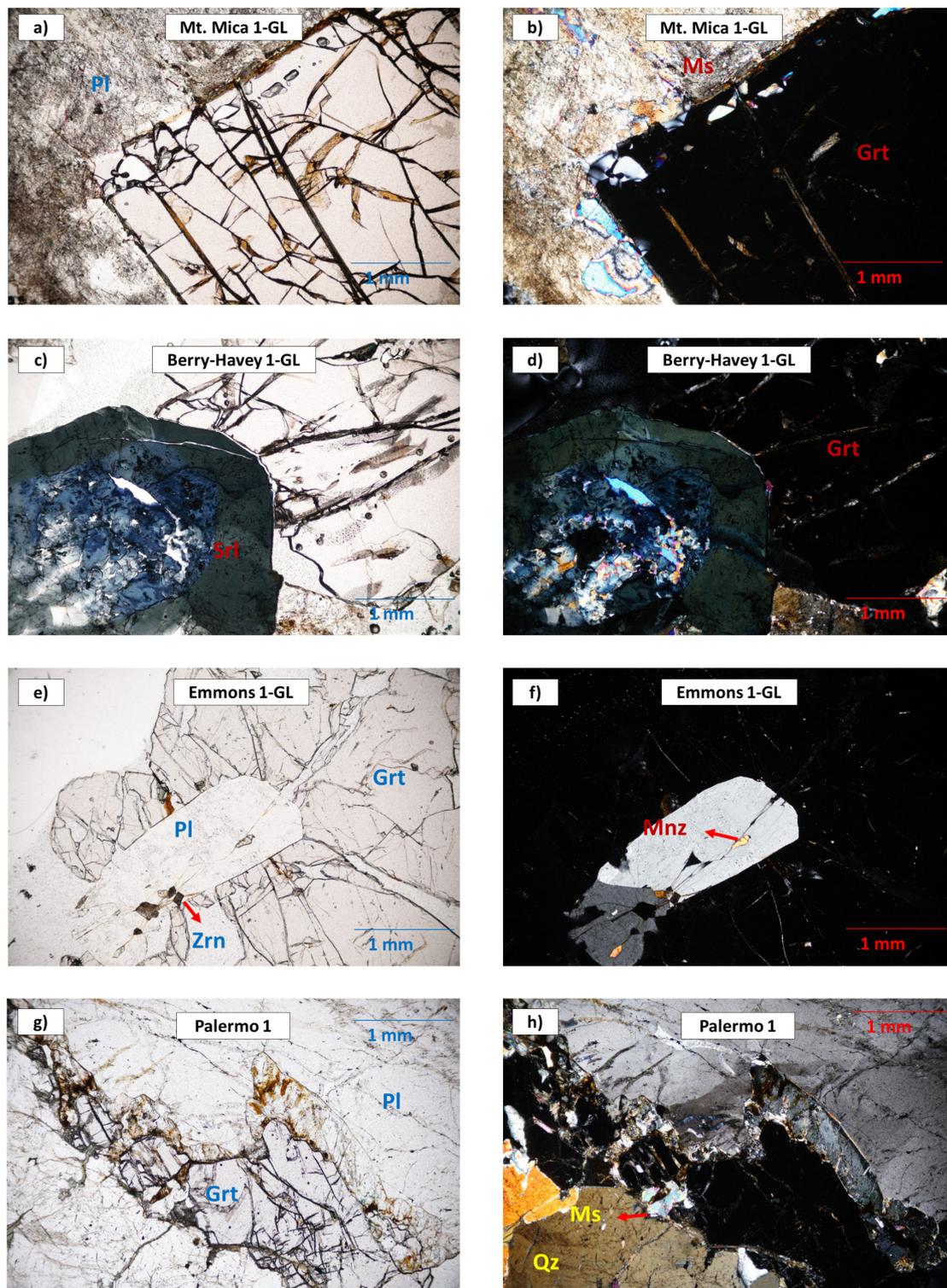
Figure 4. Photomicrographs of garnet from the evolved and intermediate pegmatites. Left: plane-polarized light; right: crossed-polarized light. Abbreviations according to [37]: plagioclase (Pl), muscovite (Ms), garnet (Grt), schorl (Srl), zircon (Zrn), monazite (Mnz), quartz (Qz). (**a**,**b**) Garnet from the Mt. Mica pegmatite showing a muscovite rim; (**c**,**d**) Tourmaline crystal from the Berry-Havey pegmatite with the core altered and replaced by very fine-grained phyllosilicates. The garnet shows chromatic zoning. It grows around a tourmaline prism; (**e**,**f**) Garnet crystal from the host migmatite of the Emmons pegmatite, growing around a plagioclase crystal. The plagioclase shows monazite and zircon inclusions; (**g**,**h**) Subhedral garnet from the intermediate zone of Palermo No. 1 pegmatite.

4.2. Berry-Havey

The highly evolved Berry-Havey pegmatite intrudes into a hornblende-rich amphibolite and is crossed by numerous mafic dykes. The pegmatite shows well-developed internal zoning, including a wall zone, composed of quartz, K-feldspar, plagioclase, biotite, muscovite, and accessory garnet and schorl; a first intermediate zone composed of graphic quartz, alkali feldspars and accessory garnet, biotite, and schorl; a second intermediate zone with similar mineralogy but a markedly coarser grain size; a core margin zone mainly composed of "vuggy" albite, quartz, muscovite, schorl, and accessory green tourmaline; and a core zone showing the most complex mineralogy. This zone, constituted by different subrounded pods, is enriched in Li, P, Be, and Cs, with minerals such as lepidolite, elbaite, montebrasite, fluorapatite, Fe-Mn phosphates, and Cs-enriched beryl or morganite (Figures 5 and 6) [9].
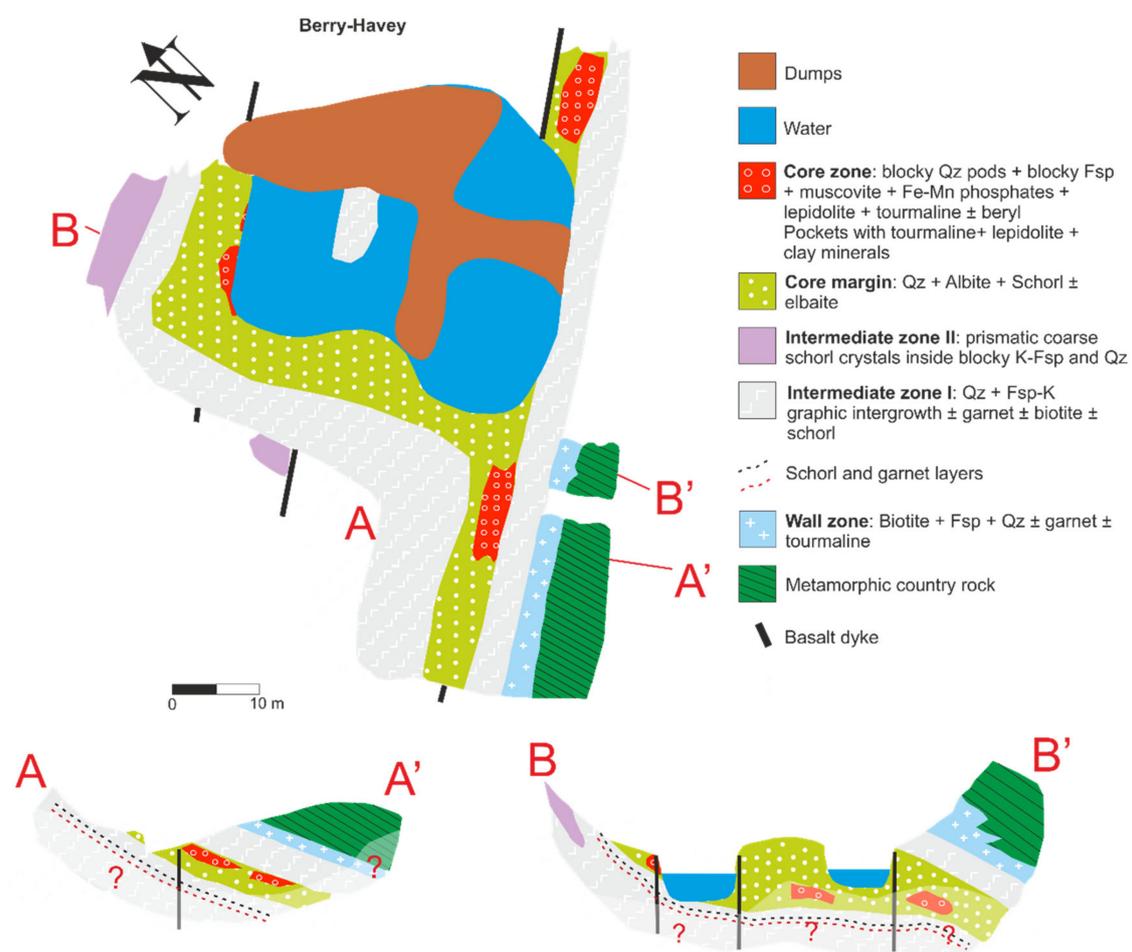
Figure 5. Map and idealized cross sections of the Berry-Havey pegmatite (modified from [9]).

Pockets appear within the core zone as isolated or interconnected miaroles. Their size ranges from a few cm^3 to ≈ 0.6 m^3. Below the core zone, a more or less continuous garnet layer appears (Figures 3b and 6). Above the garnet layer, a tourmaline layer can be found (Figure 6) [9].

In the garnet layer, garnet size is usually <4 cm in diameter, showing a subhedral to euhedral habit. Crystals are usually crossed by numerous fractures (Figure 4c,d). Often these garnets also exhibit tourmaline rims, similar to those described for the Mt. Mica garnet crystals (Figure 3b). In some areas where the garnets were dissolved, the tourmaline rims were preserved. Less commonly, garnet grows around tourmaline crystals as observed in Figure 4c. Locally garnet may also appear intimately intergrown with bluish/greenish

apatite. Some garnets present a concentric chromatic zoning, with a darker color toward the rim (Figure 4c,d).
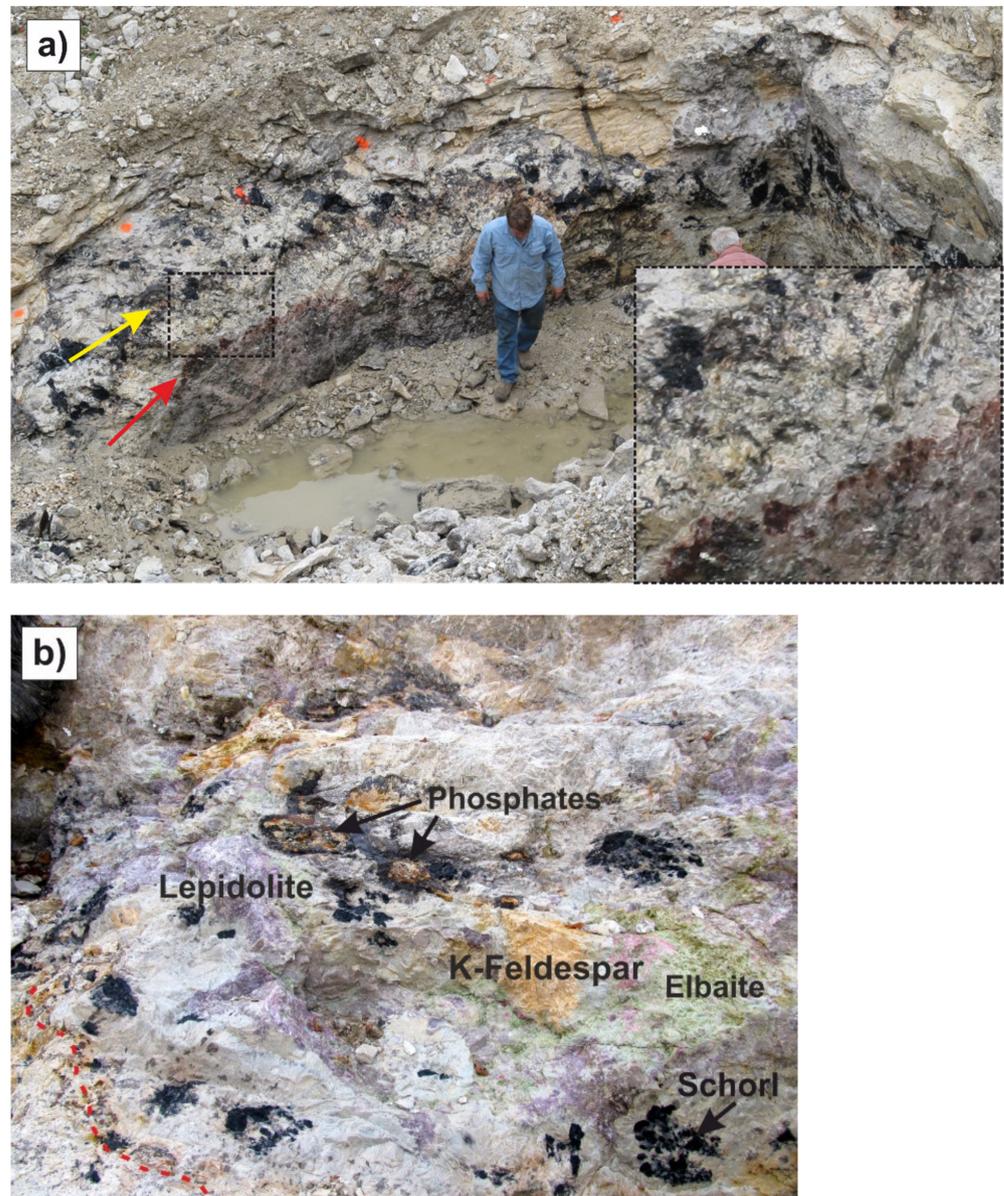
Figure 6. (**a**) General view of the Berry-Havey pegmatite. The red arrow points to the garnet layer, and the yellow arrow points to the tourmaline layer; (**b**) Lithium-rich pod from the core zone, hosted by the cleavelandite-rich core margin. The red dashed line in the left lower corner marks the garnet layer under the tourmaline layer.

4.3. Emmons

The Emmons pegmatite is a B + Cs + Ta + P ± Li-rich, highly evolved body. It intrudes into a migmatite (Figure 7), whose mineralogical composition stands out for presenting mostly amphibole with subordinate biotite. The Emmons pegmatite shows a complex internal zoning, including a wall zone, an intermediate zone, a core margin, and a core zone. In addition to these zones, pockets, replacement zones and pollucite pods can be present along the core. Lithium-Al and Fe-Mn phosphate pods may also occur in the core margin. As it has been described for the previous pegmatites, the Emmons pegmatite also exhibits a garnet layer below the core zone [38], which is double in some parts of the pegmatite (Figure 7b).
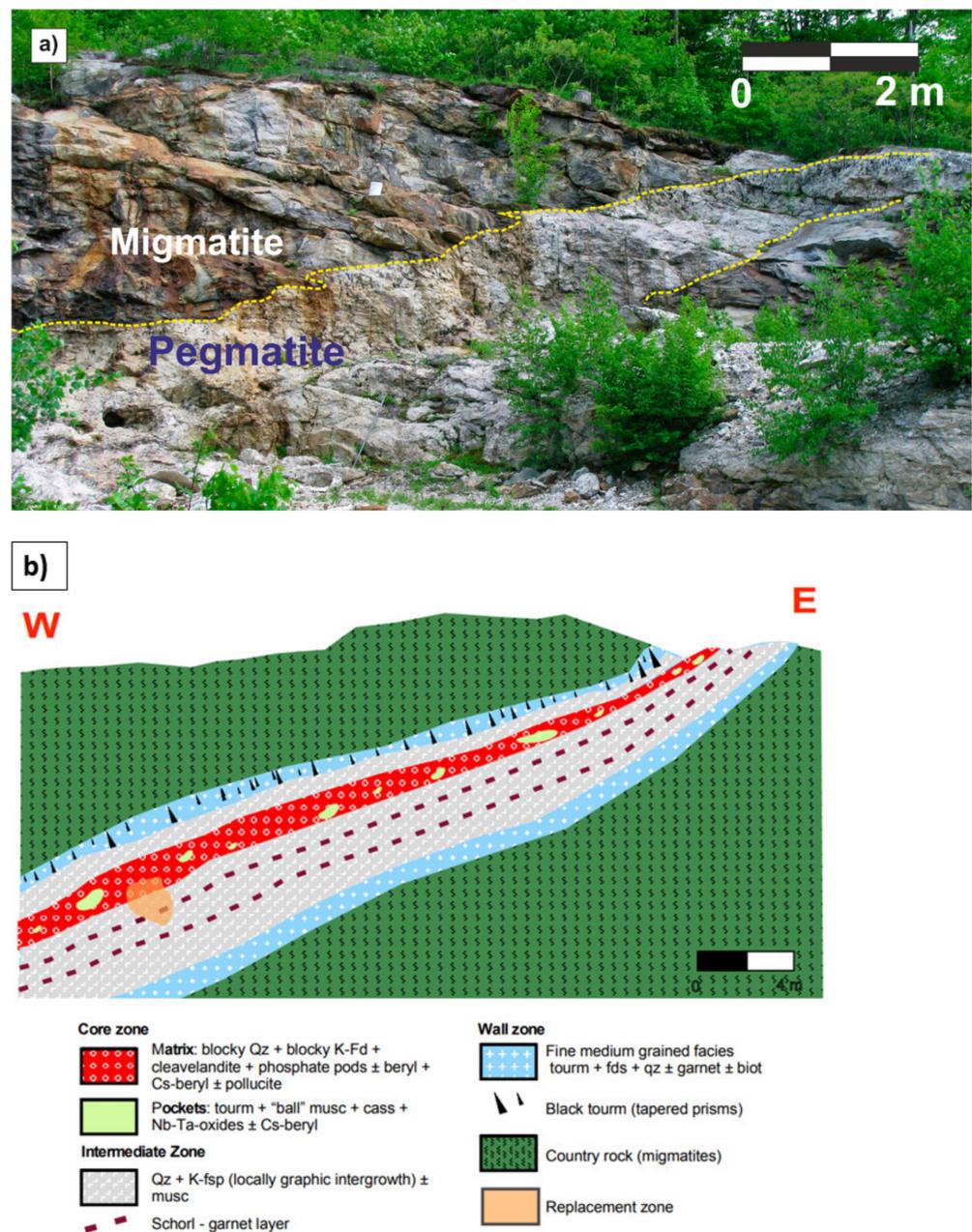
Figure 7. (**a**) General view of the Emmons pegmatite quarry, where it is possible to see the contacts between the pegmatite and the hosting migmatite; (**b**) Idealized cross-section of the Emmons pegmatite (modified from Roda-Robles in [36,38]).

In this pegmatite the garnet layer is composed of a matrix of 'blocky' plagioclase, K-feldspar, muscovite, and quartz. Along with the garnets, schorl crystals appear to grow perpendicularly to the garnet layer, showing a 'comb' texture (Figure 3c). This directional texture of tourmaline crystals is also common in the contact of the pegmatite with the hosting migmatite. Garnet crystals are generally <1 cm in size, show euhedral habit, and appear crossed by fractures (Figure 3c).

4.4. Palermo No. 1

The pegmatites of the Palermo group are hosted by sillimanite-muscovite grade metamorphic rocks (schists). These pegmatites may be classified as weakly to moderately evolved, beryl and beryl-phosphates type, rare element pegmatites, according to the classification of [39]. Palermo No. 1 is a beryl-phosphates pegmatite, with a well-developed

internal zoning, where five zones are differentiated. The border zone appears discontinuously, with a thickness below 10 cm, and is composed of quartz, muscovite, albite, and biotite. The wall zone, with a thickness ranging from 0.2 to 5 m, presents a similar composition to the border zone, although with larger grain size and the presence of schorl. The intermediate zone ranges in thickness from 3 to 25 m and is composed of quartz, albite, K-feldspar, and muscovite, and accessory garnet and tourmaline, with crystals that reach up to 30 cm in size. The core margin has a thickness below 10 m, with a great variety of grain sizes (from 2 cm to 1 m). Its composition is very similar to the intermediate zone, but this zone contains the rarest minerals of the pegmatite, among which there is a great variety of phosphates and beryl. Garnet and tourmaline are not common in the core margin. The core zone, with a thickness over 30 m, is mainly composed of quartz and K-feldspar [40].

Garnets from the Palermo No. 1 pegmatite were taken from the innermost portion of the intermediate zone. They show brownish color and subhedral habit, with sizes <2 cm in diameter. Rims of fine-grained muscovite may appear around the garnets (Figure 4g,h), whereas no tourmaline rims have been observed. Garnet crystals, which coexist with quartz, plagioclase, muscovite, and small tourmaline crystals, are crossed by numerous fractures.

4.5. Barren Pegmatites

Perham and Stop-35 are both barren pegmatites with a low fractionation degree. The Perham pegmatite intrudes into a biotite-rich amphibolite with poorly-developed internal zoning. Major minerals of the pegmatite include plagioclase, K-feldspar, quartz, muscovite, biotite, and garnet. Large schorl crystals can also be found. Garnet crystals range in size from 2 mm to 1 cm, with a subhedral habit and abundant inclusions (mainly biotite) and are crossed by numerous fractures (Figure 8a,b).

The Stop-35-pegmatite intrudes into a migmatite, and seems to correspond to a leucosome of the migmatite itself, which shows a clearly pegmatitic texture: coarse to very coarse grain size and unidirectional solidification 'comb' growth textures and graphic intergrowth. The mineralogy of the Stop-35-pegmatite is very similar to that of the Perham pegmatite, mainly including plagioclase, K-feldspar, quartz, muscovite, biotite, and garnet. In the two barren pegmatites, garnet crystals were taken from an intermediate position within the bodies.

Garnets are also present in the migmatite hosting Stop-35 pegmatite. These garnet crystals are commonly fractured, showing inclusions of other minerals such as quartz, feldspar, and biotite (Figure 8e,f). In both samples (Stop-35 pegmatite and migmatite), garnets show subhedral and anhedral habit, and, in general, their size is smaller than those described in the previous pegmatites, ranging from <1 mm to 2 mm in diameter. No chromatic zoning has been observed in the garnets of any of these samples.
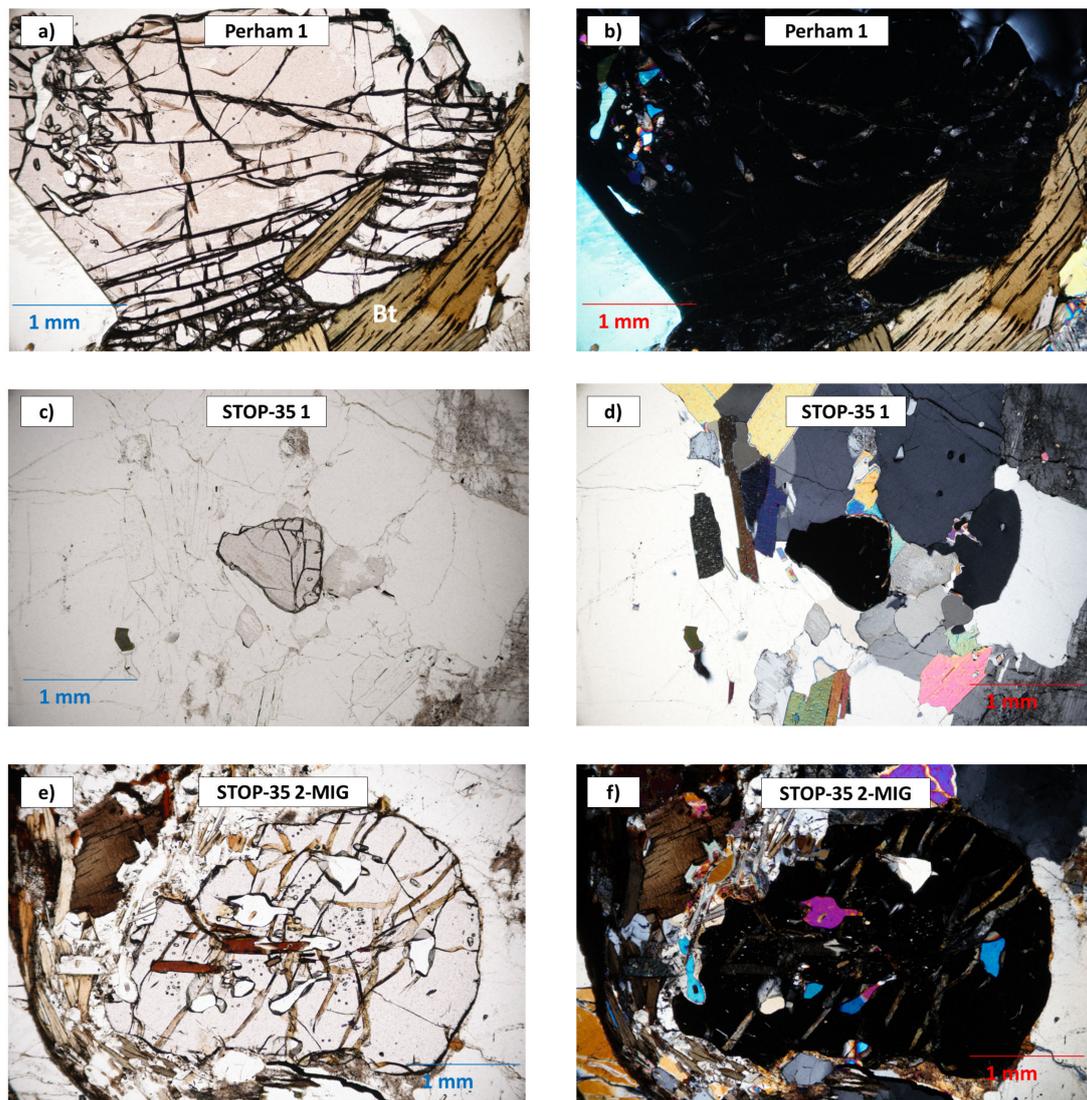
Figure 8. Photomicrographs of garnet from the barren pegmatites and the hosting migmatite. Left: plane-polarized light; right: crossed-polarized light. (**a**,**b**) Garnet from the Perham pegmatite with biotite and quartz inclusions. (**c**,**d**) Garnet from the Stop-35-pegmatite in a plagioclase, quartz and muscovite matrix. (**e**,**f**) Garnet from the Stop-35-migmatite with abundant quartz and micas inclusions.

5. Garnet Geochemistry

5.1. Major Elements

Microprobe analysis (Table 1) show that all garnets belong to the almandine-spessartine solid solution, with a higher proportion in spessartine ($Sps_{0.35–0.74}$) in garnets from the most fractionated pegmatites (13.02–31.49 wt.% MnO; 11.56–29.17 wt.% FeO), and the highest for the garnets taken close to the tourmaline layer (Figure 9a). The highest proportions in almandine ($Alm_{>0.68}$) are shown by garnets from the barren pegmatites and migmatites (2.31–10.45 wt.% MnO; 30.05–34.63 wt.% FeO). Garnets from migmatites also contain the highest contents in pyrope and andradite ($Prp_{0.07–0.15}$, $Adr_{<0.01}$). (Figure 9a).

Table 1. Representative microprobe analyses of garnets from the Oxford field pegmatites and migmatites and the Palermo No. 1 pegmatite. Values of the structural formulae normalized to 12 oxygens. Complete dataset available in Table S1 (Supplementary Materials).

| | Mt. Mica | | | | | Berry-Havey | | | Emmons | | | | Pal. | Perham | | Stop-35 | | | |
| | 1-GL | 2-GL | 3-GL | | 4-GL * | 1-GL | | 2-GL * | 1-GL | | 2-MIG | | 1 | 1 | | 1 | | 2-MIG | |
			Core	Rim		Core	Rim		Core	Rim	Core	Rim		Core	Rim	Core	Rim	Core	Rim
SiO$_2$	35.85	36.43	36.37	36.07	36.22	36.53	36.33	36.20	36.44	36.40	37.74	36.97	36.50	36.22	36.66	36.94	36.94	37.50	37.49
TiO$_2$	0.14	0.00	0.00	0.00	0.02	0.02	0.13	0.02	0.08	0.00	0.00	0.00	0.03	0.40	0.00	0.07	0.00	0.00	0.29
Al$_2$O$_3$	21.19	21.10	20.82	20.33	20.71	21.08	20.85	20.43	21.07	21.07	21.59	21.19	20.80	21.13	21.17	21.32	21.06	21.65	21.31
MgO	0.15	0.04	0.12	0.26	0.00	0.17	0.10	0.00	0.00	0.00	3.72	2.04	0.06	0.58	0.61	0.80	0.40	3.70	2.45
CaO	0.26	0.23	0.28	0.32	0.27	0.31	0.32	0.10	0.18	0.20	1.12	1.10	0.24	0.29	0.33	0.34	0.35	1.16	1.04
MnO	15.91	17.18	15.94	16.06	28.39	14.67	15.39	29.53	18.53	20.76	3.35	8.40	16.16	8.95	10.01	7.90	10.45	2.31	5.86
FeO	27.16	26.28	27.29	26.50	15.40	27.43	27.02	14.18	23.74	22.62	32.64	30.94	27.26	34.45	31.38	33.93	32.16	34.63	33.64
Na$_2$O	0.00	0.00	0.00	0.02	0.02	0.04	0.00	0.00	0.01	0.00	0.06	0.00	0.03	0.04	0.03	0.07	0.00	0.00	0.08
K$_2$O	0.00	0.00	0.01	0.01	0.00	0.00	0.00	0.00	0.00	0.00	0.01	0.01	0.00	0.00	0.00	0.00	0.00	0.00	0.00
P$_2$O$_5$ **	0.09	0.13	1.42	1.40	1.66	0.33	0.37	0.38	0.85	0.61	0.02	0.01	1.69	1.03	1.09	0.60	0.81	0.10	0.163
Total	100.7	101.3	102.2	100.9	102.6	100.5	100.5	100.8	100.9	101.6	100.2	100.6	102.7	103.0	101.2	101.9	102.1	101.0	102.3
Si	2.941	2.968	2.978	2.977	2.980	2.991	2.990	2.989	2.993	2.982	3.006	2.985	2.980	2.933	2.993	2.985	2.996	2.981	2.978
Al	2.094	2.027	2.009	2.007	2.006	2.035	2.023	1.991	2.041	2.031	2.027	2.017	2.002	2.018	2.038	2.031	2.014	2.029	1.996
Ti	0.009	0.000	0.000	0.003	0.002	0.001	0.010	0.000	0.005	0.000	0.000	0.000	0.002	0.024	0.000	0.004	0.000	0.000	0.017
P **	0.006	0.009	0.127	0.125	0.148	0.030	0.033	0.033	0.075	0.055	0.001	0.001	0.150	0.092	0.097	0.053	0.072	0.008	0.015
Fe^{2+}	1.864	1.790	1.869	1.851	1.231	1.879	1.864	0.983	1.631	1.552	2.175	2.089	1.862	2.334	2.143	2.293	2.182	2.303	2.235
Mn	1.105	1.185	1.105	1.111	1.742	1.018	1.075	2.063	1.289	1.445	0.226	0.057	1.117	0.618	0.692	0.541	0.718	0.155	0.394
Mg	0.018	0.005	0.015	0.024	0.005	0.021	0.012	0.000	0.000	0.003	0.442	0.245	0.008	0.070	0.074	0.096	0.049	0.438	0.290
Ca	0.023	0.020	0.024	0.024	0.025	0.027	0.032	0.012	0.016	0.019	0.096	0.095	0.021	0.025	0.029	0.029	0.031	0.099	0.088
Alm	60.06	58.66	61.11	59.84	32.19	62.80	62.05	38.26	54.53	50.65	72.66	68.97	60.99	74.05	71.67	76.54	72.83	76.25	73.21
Adr	0.00	0.00	0.00	0.72	0.68	0.00	0.00	0.31	0.00	0.00	0.00	0.00	0.00	0.00	0.00	0.00	0.00	0.00	0.00
Grs	0.31	0.66	0.81	0.23	0.02	0.87	0.56	0.06	0.50	0.58	3.19	3.16	0.59	0.00	0.98	0.76	1.02	3.29	2.07
Prp	0.61	0.15	0.50	1.06	0.00	0.70	0.40	0.00	0.00	0.00	14.77	8.17	0.26	2.34	2.48	3.22	1.63	14.60	9.65
Sps	36.80	39.54	36.84	37.56	65.50	34.02	35.80	60.65	43.10	47.88	7.55	19.13	37.26	20.40	23.15	18.05	23.98	5.18	13.12

GL: garnet layer; MIG: migmatite; * Closer to the tourmaline layer. ** Phosphorus data for garnets from the analyses: Mt. Mica 3-GL and 4-GL, Berry-Havey, Emmons 1-GL, Palermo, Perham and STOP-35, correspond to LA-ICP-MS analysis. End-member garnet contents given in wt.%.
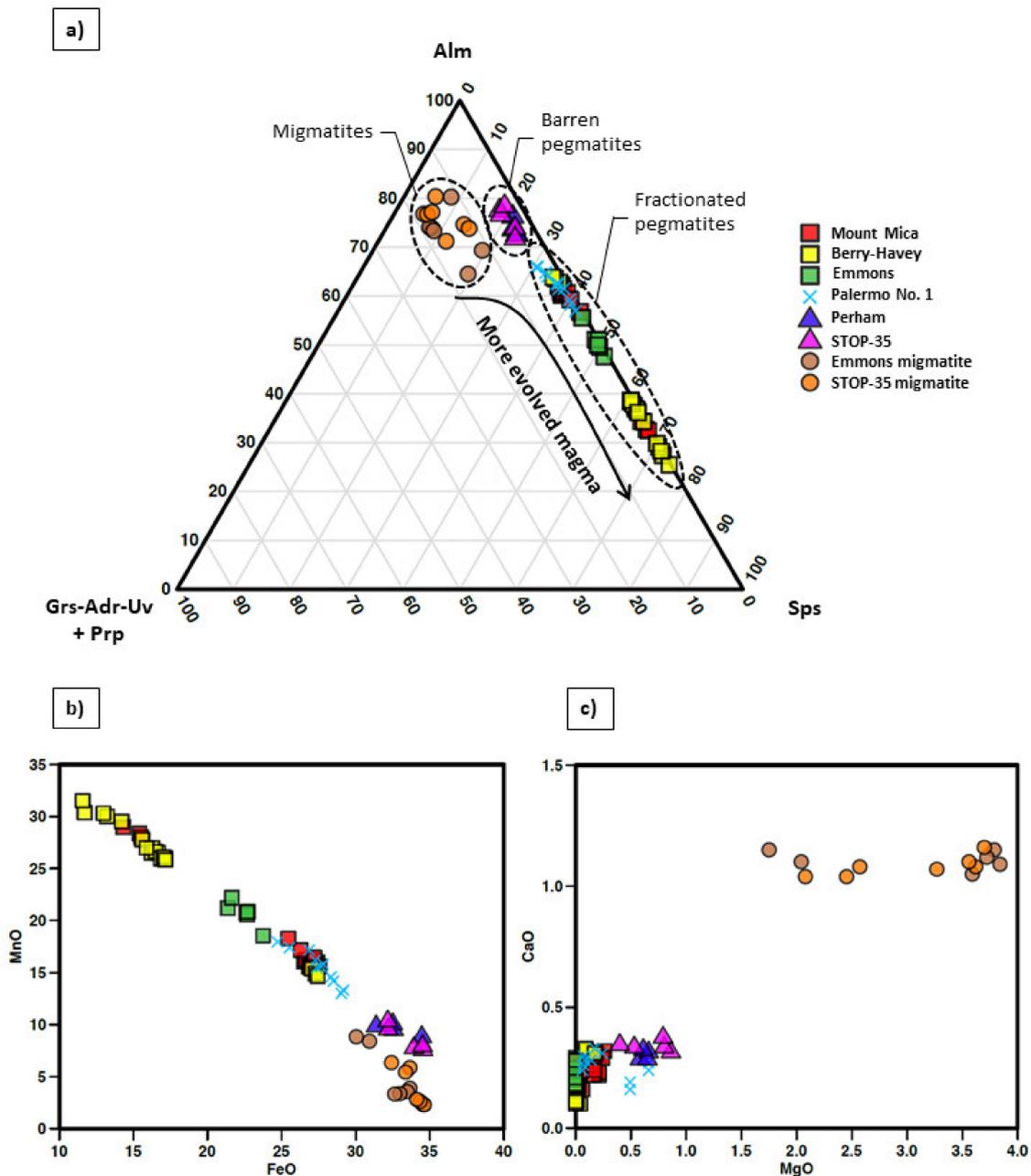
Figure 9. (**a**) Ternary diagram for the Alm—Sps—(Grs-Adr-Uv + Prp) proportions with major garnet end-members. Plots of (**b**) CaO vs. MgO and (**c**) MnO vs. FeO values of garnets from the studied pegmatites and migmatites (values given as wt.%).

The MnO and FeO values show a negative correlation, as observed in Figure 9b. For the MgO and CaO contents, such correlation is not so obvious, with the values of the migmatitic garnets moving away from the alm-sps line (Figure 9c). These trends may be also observed in Figure 9a, with increasing Ca-Mg values as the fractionation degree of the pegmatite decreases; and in Figure 9b, with a decrease in MnO parallel to the increase in FeO for the garnets from the most fractionated pegmatites (Mt. Mica and Berry-Havey) down to the barren pegmatites and migmatites.

In general, the studied garnets show a more or less marked internal chemical zoning. In all the studied garnets, Mn values generally increase from core to rim, while Fe decreases in the same sense (Figures 10a,b and 11). However, in the Berry-Havey and Emmons

pegmatites, the decrease in Fe and/or increase in Mn from core to rim is more discontinuous, sometimes with different intermediate behaviors for some of the crystals (Figure 10b–d).

Figure 10. Major element variations across garnet crystals from the studied pegmatites (**a**–**f**) and migmatites (**g**,**h**). Values in cations (apfu).
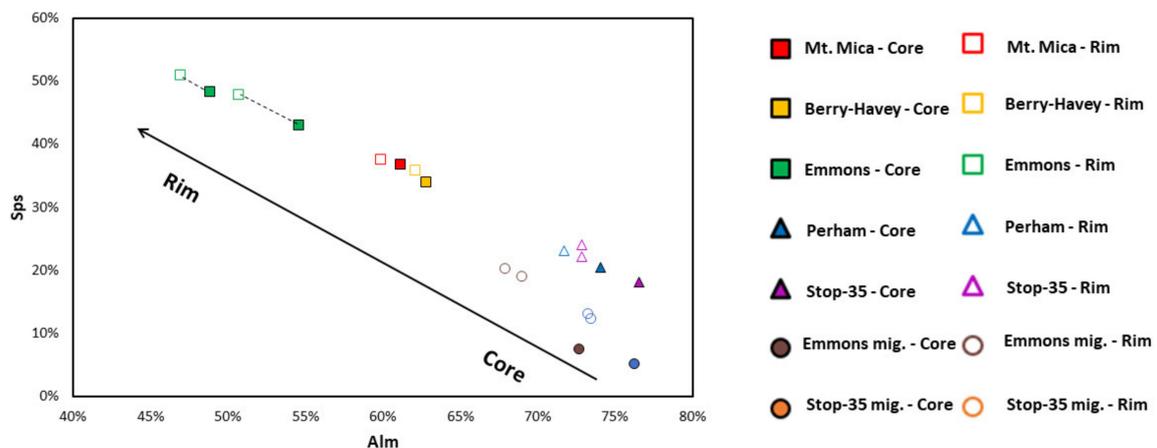

Figure 11. Plot of the almandine vs. spessartine proportions (mol %) in the analyzed garnets distinguishing the values in the core from those of the rims of the crystal.

Calcium and Mg show no significant core to rim variation in garnets from evolved pegmatites (Figure 10a–d). In contrast, in the barren pegmatites and migmatites, Mg content is slightly lower towards the garnet rim, showing a very similar trend to Fe, mainly in migmatites (Figure 10e–h).

5.2. Trace Elements

The studied garnets show a high content in some trace elements, mainly P, Li, Ti, Sc, Y, Zn, Zr, Ga, and HREE, all of them with values >5 ppm (Table 2). In addition, other elements appear with concentrations that are high enough to allow the study of their variations among the different garnets analyzed (Table 2; Figures 12–14).
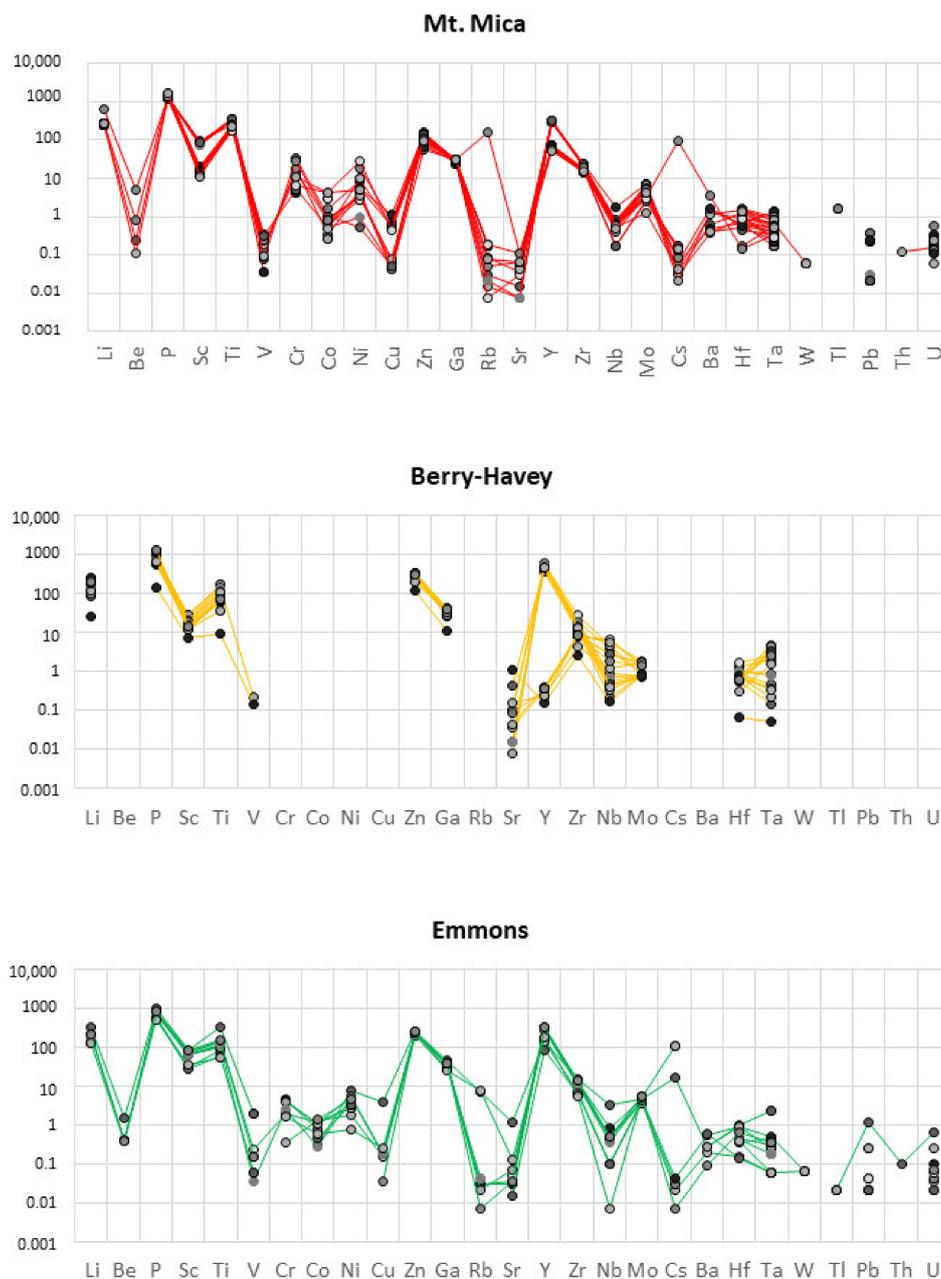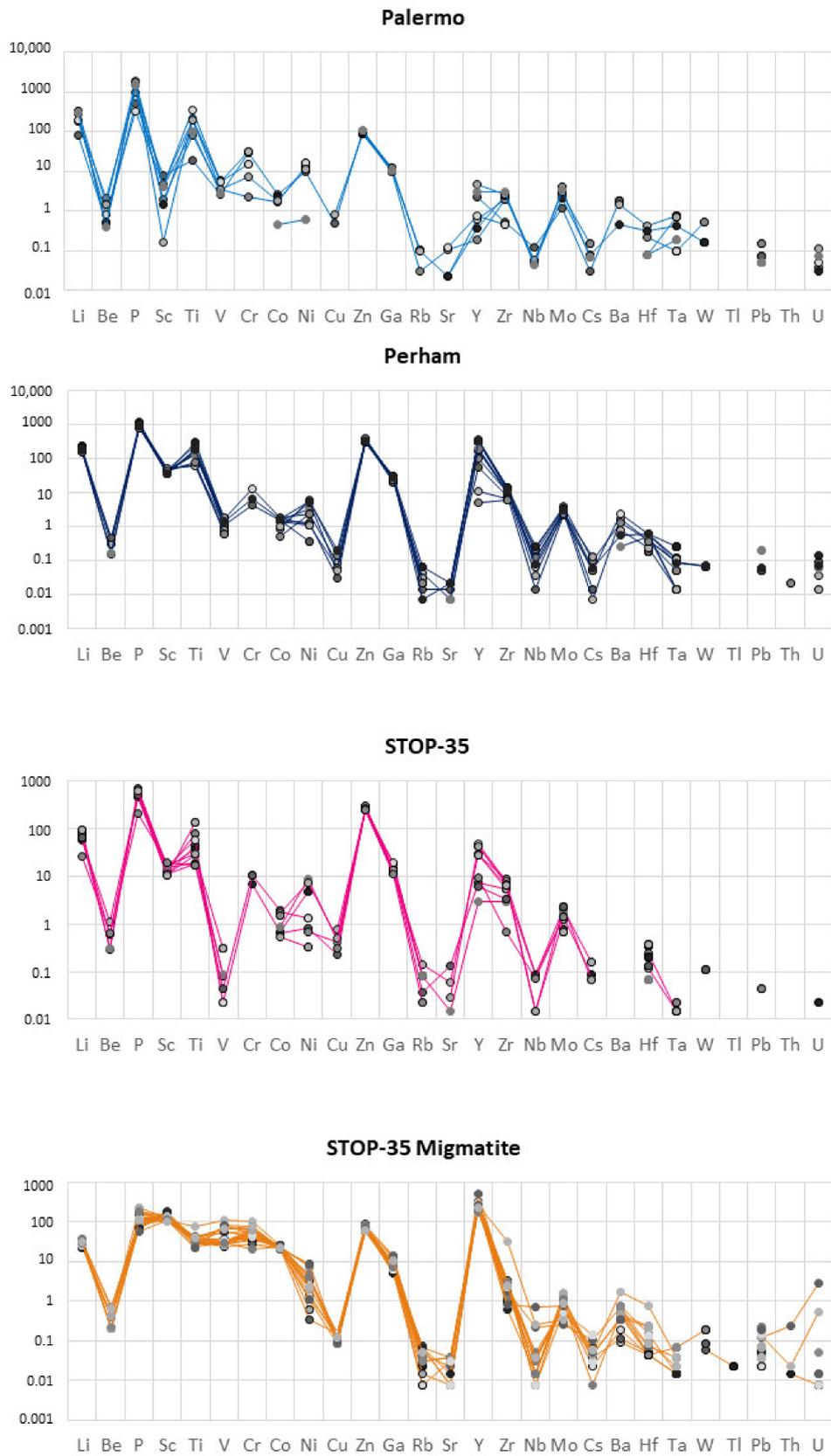

Figure 12. *Cont.*

Palermo

Perham

STOP-35

STOP-35 Migmatite

Figure 12. Trace elements spider diagrams for the garnets from the studied pegmatites.

Table 2. Representative LA-ICP-MS analyses of garnets from the Oxford field pegmatites and migmatites and the Palermo No. 1 pegmatite. n.a. not analyzed. Values in ppm. Complete dataset available in Table S2 (Supplementary Materials).

	Mt. Mica				Berry-Havey				Emmons		Palermo		Perham		Stop-35			
Sample	**3-GL**		**4-GL ***		**1-GL**		**2-GL ***		**1-GL**		**1**		**1**		**1**		**2-MIG**	
	Core	Rim	Core	Rim	Core	Rim	Core	Rim	Core	Rim	Core	Rim	Core	Rim	Core	Rim	Core	Rim
Li	277	272	255	267	166	90	244	126	213	123	329	82	188	201	80	97	36.5	24.9
Be	n.a.	n.a.	n.a.	n.a.	n.a.	n.a.	n.a.	n.a.	n.a.	0.38	n.a.	0.54	n.a.	0.43	n.a.	0.29	0.20	n.a.
P	1267	1228	1422	1462	973	577	1394	671	751	546	1881	499	915	976	682	724	92	186
Sc	88	79	16.1	16.8	26.9	18.0	13.6	19.5	71	27.3	0.16	7.8	36.0	36.9	16.1	13.6	108	139
Ti	339	323	236	210	174	80	66.4	111	134	60	207	18.8	173	183	57	78	75	37.0
V	n.a.	0.13	0.25	0.19	n.a.	n.a.	n.a.	n.a.	0.22	0.06	5.3	2.6	1.7	1.0	0.02	n.a.	114	32.3
Cr	n.a.	17.8	n.a.	10.9	n.a.	n.a.	n.a.	n.a.	1.9	n.a.	31.5	28.6	13.1	n.a.	n.a.	10.5	101	59
Co	0.89	0.44	1.7	n.a.	n.a.	n.a.	n.a.	n.a.	1.1	0.46	n.a.	2.7	1.9	1.6	1.9	n.a.	25.5	23.2
Ni	3.5	4.2	8.4	n.a.	n.a.	n.a.	n.a.	n.a.	2.7	3.3	n.a.	9.4	1.1	1.2	1.4	0.68	4.0	1.9
Cu	0.08	0.04	n.a.	n.a.	n.a.	n.a.	n.a.	n.a.	n.a.	n.a.	0.80	0.49	n.a.	0.03	n.a.	0.43	0.12	n.a.
Zn	129	152	135	124	295	331	345	306	224	243	88	102.7	346	311	274	248	75	74
Ga	29.9	28.3	28.7	28.5	33.4	27.0	41.9	29.1	37.5	27.3	12.5	10.2	26.8	26.8	19.2	18.4	12.6	8.2
Rb	n.a.	0.13	0.17	n.a.	n.a.	n.a.	n.a.	n.a.	n.a.	n.a.	0.09	0.10	n.a.	0.01	0.08	0.08	0.06	0.06
Sr	n.a.	0.06	n.a.	0.043	0.101	n.a.	n.a.	n.a.	0.05	0.01	0.02	n.a.	0.02	0.01	n.a.	n.a.	n.a.	n.a.
Y	322	294	68	75	588	388	0.223	479	308	84	0.593	2.3	299	375	48.5	27.9	262	188
Zr	19.7	22.7	15.4	16.1	28.1	11.7	8.5	13.8	12.3	6.4	1.9	0.51	11.5	14.7	7.8	9.1	31.2	3.1
Nb	0.73	0.58	0.66	0.39	4.9	0.21	6.3	0.40	0.46	0.10	n.a.	0.12	0.06	0.16	0.01	n.a.	0.26	0.01
Mo	5.6	5.5	3.8	3.5	0.87	0.80	1.6	0.88	5.4	4.0	4.0	1.2	2.1	3.4	1.2	1.3	0.351	1.2
Cs	0.02	n.a.	n.a.	n.a.	n.a.	n.a.	n.a.	n.a.	n.a.	n.a.	1.4	0.03	0.05	0.01	n.a.	n.a.	0.05	0.04
Ba	1.2	n.a.	n.a.	0.42	n.a.	n.a.	n.a.	n.a.	n.a.	0.61	0.42	1.8	2.4	n.a.	n.a.	n.a.	1.7	0.40
Hf	0.90	1.4	0.17	0.52	1.7	0.55	0.75	0.74	0.45	0.14	0.74	n.a.	0.59	0.54	0.12	0.25	0.75	0.22
Ta	0.673	0.57	0.58	0.23	2.6	0.14	5.0	0.35	0.30	0.06	n.a.	n.a.	0.11	0.12	n.a.	0.01	0.04	n.a.
W	n.a.	n.a.	n.a.	n.a.	n.a.	n.a.	n.a.	n.a.	n.a.	n.a.	n.a.	n.a.	n.a.	n.a.	n.a.	n.a.	n.a.	n.a.
Tl	n.a.	n.a.	n.a.	n.a.	n.a.	n.a.	n.a.	n.a.	n.a.	n.a.	n.a.	n.a.	n.a.	n.a.	n.a.	n.a.	n.a.	n.a.
Pb	n.a.	n.a.	0.36	n.a.	n.a.	n.a.	n.a.	n.a.	0.04	0.02	n.a.	0.07	n.a.	n.a.	n.a.	n.a.	0.13	0.07
Th	n.a.	n.a.	n.a.	n.a.	n.a.	n.a.	n.a.	n.a.	n.a.	n.a.	n.a.	n.a.	n.a.	n.a.	n.a.	n.a.	0.02	n.a.
U	0.30	0.19	0.11	0.06	n.a.	n.a.	n.a.	n.a.	0.06	0.02	n.a.	n.a.	0.01	0.10	n.a.	0.02	0.52	n.a.
La	n.a.	0.10	0.06	n.a.	0.01	n.a.	n.a.	n.a.	0.05	n.a.	n.a.	n.a.	0.04	n.a.	n.a.	n.a.	0.02	0.01
Ce	0.02	0.04	n.a.	n.a.	0.06	n.a.	n.a.	0.00	n.a.	n.a.	0.07	n.a.	n.a.	n.a.	n.a.	n.a.	n.a.	0.03
Pr	n.a.	n.a.	n.a.	n.a.	0.010	0.00	n.a.	0.00	0.02	n.a.	0.03	n.a.	0.04	0.02	n.a.	n.a.	0.11	n.a.
Nd	0.26	0.12	0.58	n.a.	0.12	0.05	n.a.	0.06	n.a.	n.a.	0.36	0.38	n.a.	0.14	n.a.	n.a.	n.a.	0.37

Table 2. *Cont.*

| Sample | Mt. Mica | | | | Berry-Havey | | | | Emmons | | Palermo | | Perham | | Stop-35 | | | |
| | 3-GL | | 4-GL * | | 1-GL | | 2-GL * | | 1-GL | | 1 | | 1 | | 1 | | 2-MIG | |
	Core	Rim	Core	Rim	Core	Rim	Core	Rim	Core	Rim	Core	Rim	Core	Rim	Core	Rim	Core	Rim
Sm	115	0.82	0.99	1.7	2.3	1.6	n.a.	1.9	0.92	0.53	n.a.	n.a.	0.36	0.39	n.a.	n.a.	n.a.	0.32
Eu	n.a.	0.02	n.a.	0.10	0.00	0.00	n.a.	0.00	n.a.	n.a.	n.a.	n.a.	0.03	n.a.	0.12	n.a.	0.03	0.03
Gd	5.4	5.1	3.8	7.1	21.4	18.0	n.a.	19.3	8.9	4.5	0.45	0.49	1.7	3.4	n.a.	1.1	3.5	2.9
Tb	4.3	4.4	2.4	2.7	13.3	11.3	0.00	11.9	7.1	3.6	n.a.	0.21	3.0	2.8	0.40	0.13	2.0	1.7
Dy	40.4	46.7	19.5	18.3	111	86	0.02	96	56	20.2	0.13	0.55	35.9	36.6	4.5	3.1	30.4	24.9
Ho	8.6	7.6	1.5	1.4	14.3	8.8	n.a.	10.8	7.3	1.8	0.04	0.11	8.2	11.0	1.2	0.84	11.7	7.5
Er	23.5	19.9	2.0	1.5	27.5	12.9	0.01	17.8	14.7	1.7	n.a.	0.15	28.0	45.3	5.6	2.9	38.8	19.9
Tm	3.5	3.1	0.05	0.30	3.35	1.2	n.a.	2.0	1.7	0.20	n.a.	0.07	4.8	10.8	1.5	0.72	7.75	2.7
Yb	28.3	18.2	0.48	0.24	18.2	4.9	0.02	9.6	11.4	0.18	n.a.	0.94	36.6	103	13.7	7.4	68.6	15.3
Lu	2.6	1.7	n.a.	n.a.	1.5	0.32	0.00	0.73	1.1	0.03	n.a.	0.06	3.8	14.2	1.5	0.81	9.8	1.3

GL: garnet layer; MIG: migmatite; * Closer to the tourmaline layer.
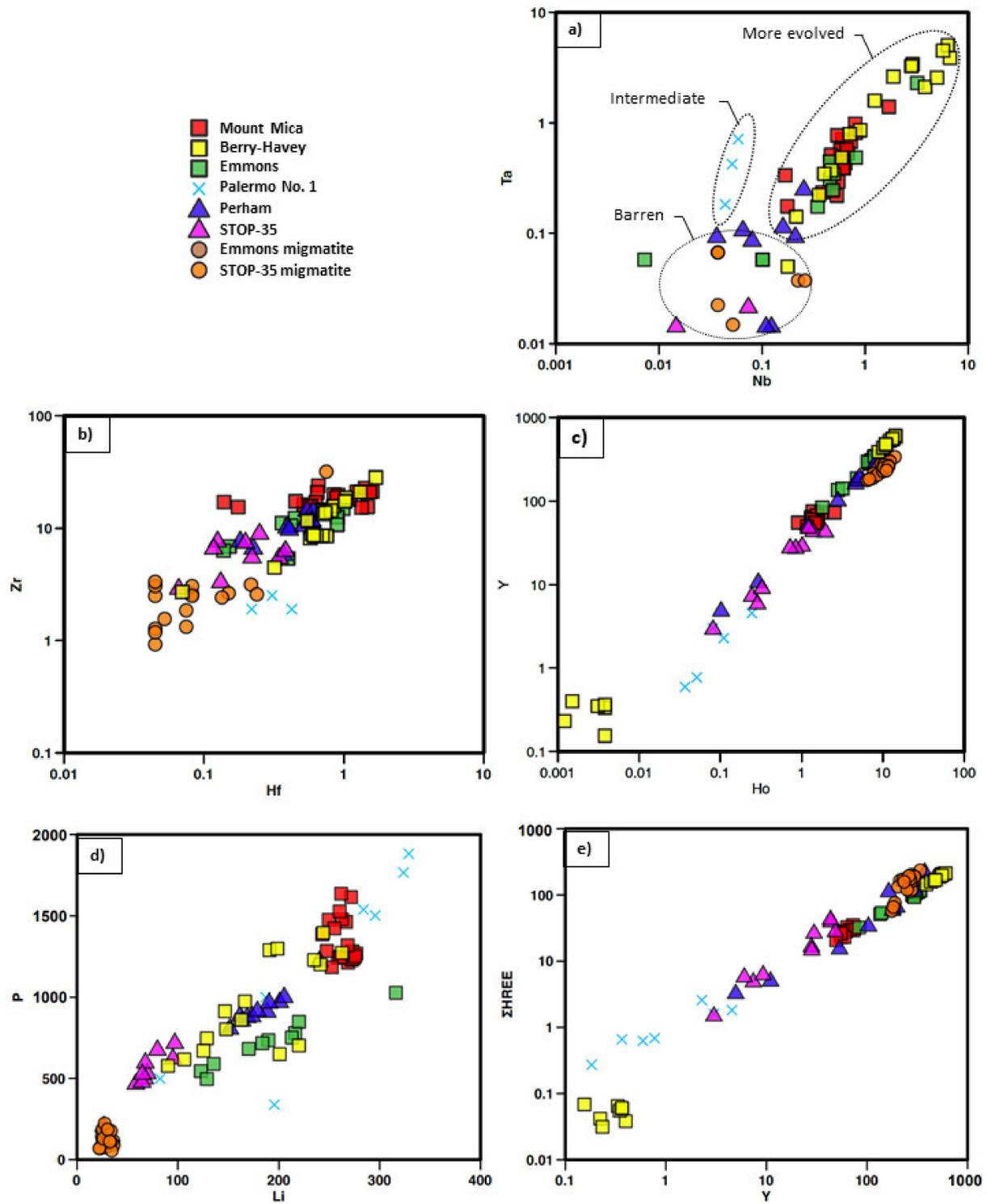
Figure 13. Trace elements binary plots for garnet samples analyzed by LA-ICP-MS (values in ppm). (**a**) Nb vs. Ta; (**b**) Hf vs. Zr; (**c**) Ho vs. Y; (**d**) Li vs. P; and, (**e**) Y vs. ΣHREE.
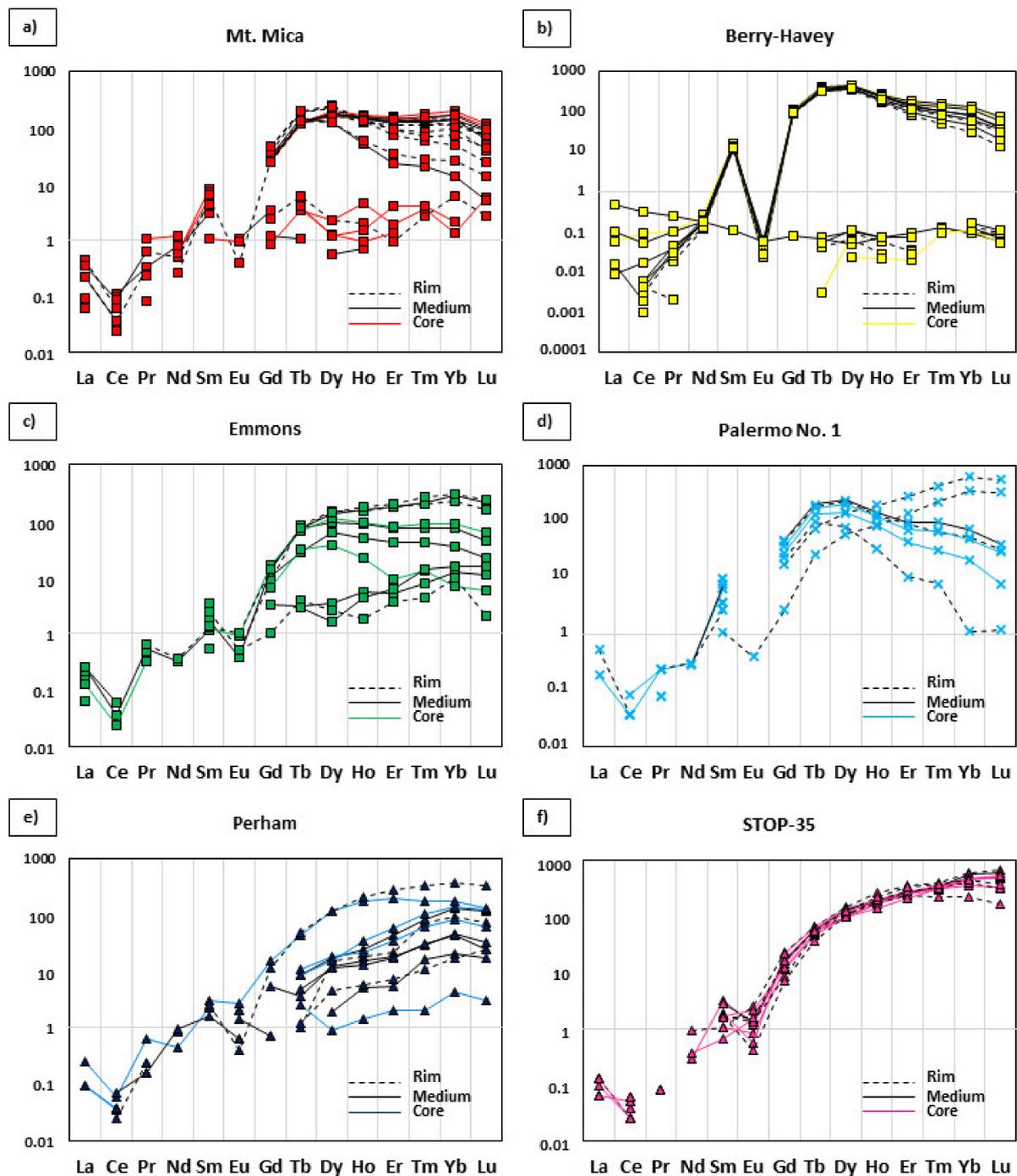
Figure 14. Chondrite normalized [41] REE spider diagrams for garnets from the different pegmatites: (**a–c**) evolved pegmatites; (**d**) intermediate pegmatite; and (**e**,**f**) barren pegmatites. Differences in the connecting lines indicate the zone of the crystal where the analyses were done (core, intermediate, or rim).

The spider diagrams of all garnets from pegmatitic rocks show overall a very similar pattern, in clear contrast to that of the migmatitic sample, which is richer in Sc, V, Cr, and Co and poorer in Li, P, Zn, Ga, Zr, and Hf than the pegmatitic garnets (Figures 12 and 13). Nevertheless, garnets from Mount Mica and Emmons pegmatites show some abnormally higher Cs and Rb values (Figure 12), which could be attributed to the microinclusions of Cs- and Rb-rich minerals such as pollucite, found inside fractures of some of the garnet crystals from the garnet layer. In addition, some analyses corresponding to garnets from Berry-Havey show lower Y contents, whereas those from Palermo No. 1 differ in the Y and

Sc contents, also with some lower values. There is a clear positive correlation between the pairs of elements Nb-Ta, Y-Ho, Zr-Hf, and P-Li (Figure 13). The highest contents in Nb and Ta correspond to the garnets associated with the most fractionated pegmatites, with intermediate values for those from the Palermo No. 1 pegmatite, which presents a lower fractionation degree; and with the lowest values in the barren pegmatites, which appear in the same ranges as the migmatitic garnet from Stop-35-migmatite (Figure 13a).

Other trace element pairs show a positive correlation, but seem to be unrelated to the fractionation degree of the pegmatite (Figure 13c–e). Garnets associated with migmatites are the richest in HREE and Y, and the poorest in Zr, Hf, P, and Li. Garnets associated with more fractionated pegmatites tend to show higher contents in these last elements (Figures 12 and 13b,d). Heavy rare earths (HREE) show a positive correlation with Y (Figure 13e) and their content shows no obvious relationship with the pegmatite fractionation degree; in particular, both high and low HREE contents occur in garnets from the Berry-Havey pegmatite (Table 2; Figure 13e).

The REE content and distribution in the studied garnets may be observed in Table 2 and Figure 14. One sample with garnet closely intergrown with apatite from the Berry-Havey pegmatite, shows a strong REE depletion. The rest of the samples show a marked negative Eu anomaly, and a general increase in the REE content from light to heavy, as is common in this mineral.

Certain differences are observed in the HREE spectra (Tb-Lu), in relation to the fractionation degree of the corresponding pegmatite. The garnets associated with the most fractionated pegmatites have a flat or negative slope (Figure 14a–c). Garnets from the intermediate Palermo No. 1 pegmatite display both negative and positive slopes (Figure 14d), and garnets from the barren pegmatites always present positive slopes for HREE (Figure 14e,f).

REE contents of the studied garnets do not show any zoning pattern from core to rim of the crystals (Figure 15). On the contrary, in the evolved pegmatites P, Ti, Y, Zr, Hf, Nb, and Ta, show a core to rim zonation. Mt. Mica, Berry-Havey, and Emmons garnets show a continuous decrease for Ta and Nb (Figure 15a–c), and with a gradual depletion in the rest of the elements in Berry-Havey and Emmons (Figure 15b,c). In Palermo No. 1 (Figure 15d) zoning patterns of garnet are not so clear, and only a decrease of P and Ti towards the rim is observed. Garnets from the barren pegmatites (Figure 15e,f) do not show a significant variation in the trace elements content from core to rim.
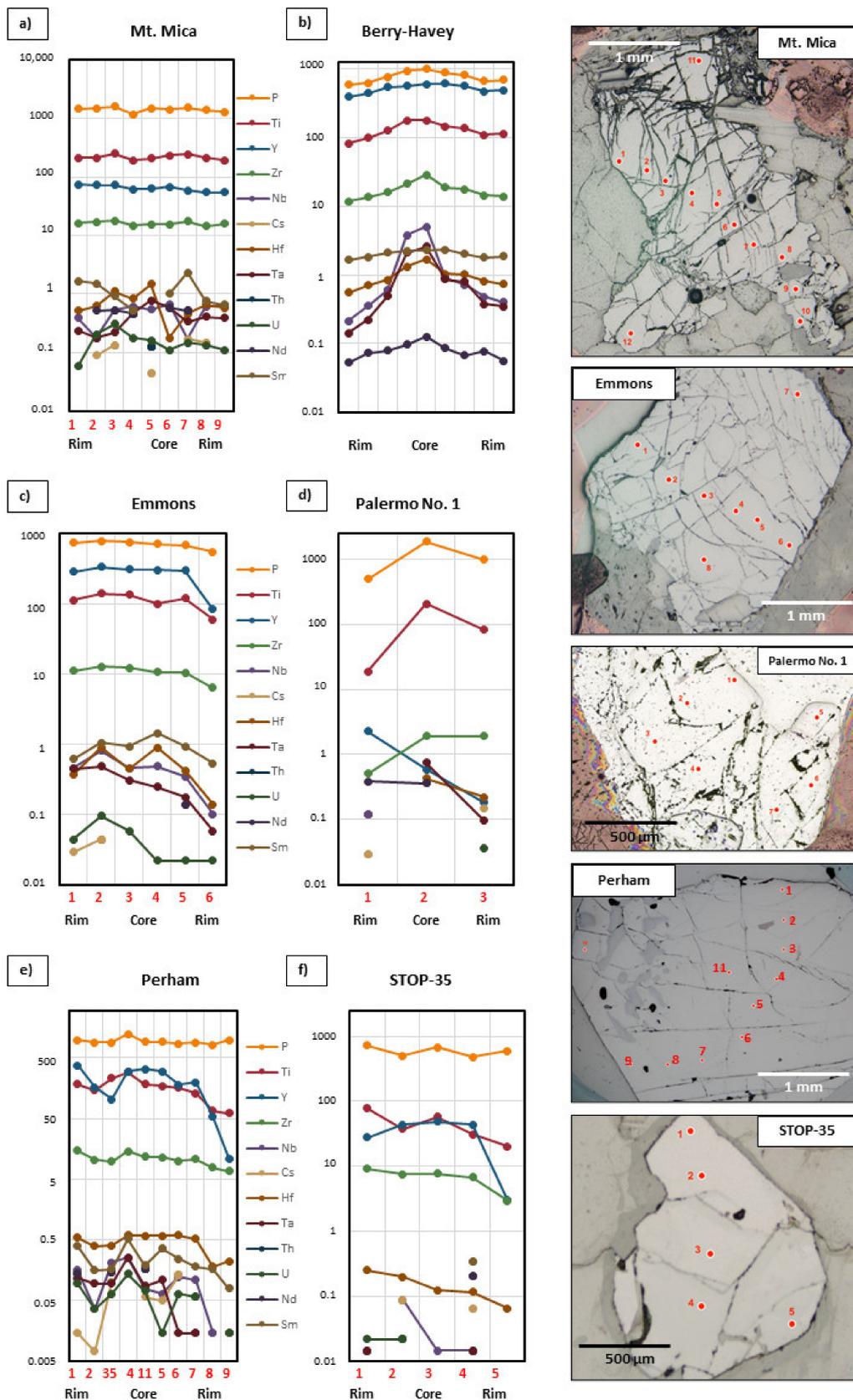
Figure 15. Trace element zoning diagrams. On the right side are shown the photomicrographs of the analyzed points in each garnet of the fractionated pegmatites (**a**–**c**), intermediate pegmatite (**d**); and barren pegmatites (**e**,**f**).

6. Discussion

6.1. Garnet Chemistry Controls

6.1.1. Major Elements

The composition of magmatic garnets is mainly controlled by two factors: (i) the composition of the magma from which they crystallize (e.g., [42]); and, (ii) the competing effects of coexisting minerals (e.g., [43]). As shown in Figures 9a,b and 11, all the garnets of the studied pegmatites belong to the alm-sps solid solution, with very low proportions of the Ca- and Mg-rich components (the highest values corresponding to garnets from the barren pegmatites), indicating that the parental pegmatitic magma was richer in Fe-Mn than in Ca-Mg. As previously described for other pegmatites (e.g., [15,44]), garnets associated with the barren pegmatites are more enriched in FeO than in MnO, in contrast to those of the more fractionated pegmatites, where the spessartine component becomes more important (Figures 9a,b and 11). On the other hand, biotite, the main Mg-carrier in these rocks, is much more abundant in the barren pegmatites than in the intermediate and evolved ones, where it may be nearly absent. Tourmaline composition also reflects the fractionation degree, with Fe-rich schorl (±Mg) occurring in the barren pegmatites and the more Na ± Li-rich schorl-elbaite tourmaline in the evolved ones. Finally, Fe-Mn-phosphates, if present, are richer in Fe than Mn in the less fractionated pegmatites. Therefore, taking into account the mineral paragenesis of the pegmatites with different fractionation degrees, together with the higher Fe and Mg content in the garnet from the barren bodies, strongly supports the inference that barren pegmatites crystallized from magmas relatively richer in ferromagnesian elements.

The influence of other minerals, which compete for common elements with garnet, is reflected in Mt. Mica and Berry-Havey garnet layers in the noticeable chemical differences observed between garnets occurring proximal to the tourmaline layer, compared with those growing distal from it. As schorl crystallizes, it preferentially consumes Fe, depleting the magma in this element, and the proximal garnets become richer in Mn. The absence of garnet in the central, more fractionated areas of these pegmatitic bodies has also been attributed to the precipitation of Fe-Mn phosphates [45–47], which begins when the P content in the melt is high enough. The formation of these phosphates, which incorporate significant amounts of Fe and Mn, may be sufficient to cause the destabilization of the garnet.

Magnesium preferentially partitions into biotite, present only in the wall zone of the most fractionated pegmatites. This way pegmatitic melts become depleted in Mg from the first crystallization stages and, consequently, its content in garnet from the garnet layer would necessarily be low.

The Ca content may be controlled by minerals such as plagioclase, which is abundant in pegmatites and, to a lesser extent, by the presence of apatite, both Ca-bearing minerals. The plagioclase richest in Ca is the first to crystallize from the pegmatite melt, in the most external zones of the pegmatites (wall and intermediate zones), thus rapidly depleting the melt in this element.

Therefore, the content in major elements of the analyzed garnets may be determined, firstly, by the original composition of the pegmatitic melt, poorer in Mg, Ca, and Fe as the fractionation degree increases and, secondly, by the competition for these elements from other coexisting minerals: schorl and biotite for Fe and Mg, Fe-Mn phosphates for these elements; and plagioclase and apatite for Ca.

The main substitution mechanism in the studied garnets is the exchange between Fe and Mn in cubic positions ($Fe^{2+}_{-1}Mn^{2+}_{1}$) owing to their similarity in ionic size and charge. As Fe is the smallest cation, it is preferentially incorporated into the garnet structure and depletes the magma in that element, allowing for Mn enrichment toward the rim. The major element zoning at crystal level (Figure 10) follows this same pattern. The Mn enrichment towards the rim, typical of magmatic garnets [48], occurs in most analyzed samples (Figure 11). There is an exception in one of the garnet crystals from the Emmons pegmatite that shows a final minor decrease in the Mn content (Figure 10c). The crystallization of the

earliest Mn-rich phosphate crystals, abundant in the core zone of this pegmatite, could be involved in this anomalous trend, decreasing the available Mn in the melt, as it has been discussed above.

6.1.2. Trace Elements

Trace element compositional variations in garnet are related to more complex mechanisms than a simple cationic Fe-Mn substitution. The CHARAC field (Charge-and-Radius-Controlled) shows the area where the distribution of trace elements may be controlled exclusively by the ionic radius and charge parameters. According to [49], the further away the samples are from the CHARAC field (for evolved magmatic systems), the greater the fractionation degree of the melt, which is usually associated with a higher fluid activity. In Figure 16, it may be observed that only samples from the Stop-35 barren pegmatite and its hosting migmatite, and those from the Palermo No. 1 intermediate pegmatite, fall within the CHARAC field. As the fractionation degree increases, data plot further away from the CHARAC field. Therefore, most of the studied garnets show non-CHARAC behavior, especially those from the evolved pegmatites, which could be attributed to a higher fractionation degree of the associated pegmatitic melts, presumably having a higher fluid activity, as suggested by [49].
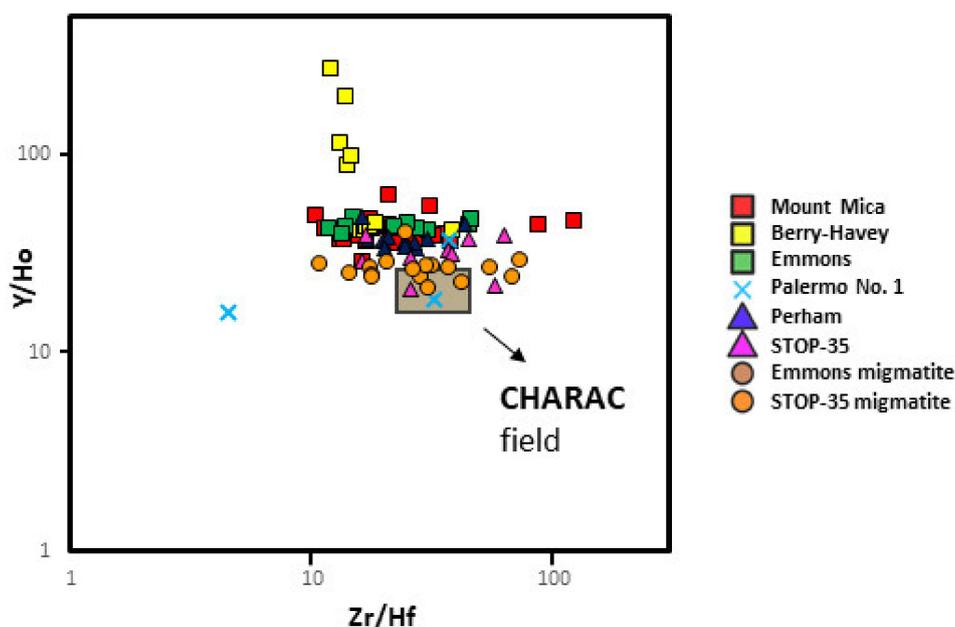

Figure 16. Plot of the values Y/Ho vs. Zr/Hf for the studied garnets. The grey rectangle shows the CHARAC field for evolved magmatic systems as suggested by [49].

The positive correlation of Li and P in Figure 13d may be attributed to a variant of the coupled substitution model proposed by [50]: $R^{1+}P(R^{2+}Si)_{-1}$, where R^{1+} = Na^{1+} (1.18 Å, in VIII coordination) is exchanged by R^{2+} = Ca^{2+} (1.12 Å) or Mn^{2+} (0.96 Å), both in VIII coordination, and Si^{4+} (0.26 Å), in IV coordination. In the present work, we propose that Li^{1+} (0.92 Å) in VIII coordination is is interchanged with Fe^{2+} and Mn^{2+}. Sodium could be more easily incorporated in minerals such as plagioclase and/or schorl. The substitution $(Fe^{2+}, Mn^{2+})_{-1}Si_{-1}Li_1P_1$, may be possible without generating a negative or positive charge excess, and it may allow both cations (Li and P) to increase in equal proportions in the garnet composition, as it is reflected in Figure 13d.

For the pair of elements Y and Ho (Figure 13c), both with the same charge and quite similar ionic radii (1.019 Å, 1.015 Å, respectively) the following substitution model may be proposed: $[R^{3+}]_2[vac]_1[R^{2+}]_{-3}$, where two trivalent atoms of Y^{3+} and/or Ho^{3+}, are exchanged for three divalent atoms of Mn^{2+} (0.96 Å) and/or Fe^{2+} (0.92 Å) in cubic

positions, which generates vacancies in those positions. Having such similar geochemical characteristics, both Y and Ho may be incorporated into the garnet structure in the same proportions, following the mechanism described here, and causing the positive correlation observed in Figure 13c.

A positive correlation between Y and ΣHREE values is observed for the analyzed garnet crystals (Figure 13e). However, a relationship between the contents in those elements and the fractionation degree of the associated pegmatites is not evidenced. In addition, significant variations are observed in the individual REE spectra for garnets from the same pegmatite (Figure 14a–d). This, together with the lack of correlation between the Y and ΣHREE contents and the fractionation degree of the associated pegmatite, may be related to the presence of other minerals that usually incorporate Y and REE into their structure in important quantities—such as monazite-Ce, xenotime-Y, zircon, and/or apatite [51]—which have been observed as individual crystals in some of the studied samples (Figure 4e,f), and/or as microinclusions in other minerals of these pegmatites (e.g., [6]). An example of the influence of these minerals on the content and distribution of REE and Y in the studied garnets is observed in the sample of garnet intergrowth with apatite in the garnet layer of the Berry-Havey pegmatite. In this sample, the REE and Y may have preferentially entered into the structure of the apatite, thus coexisting garnet is depleted in these elements. This would explain the poorly defined chondrite normalized REE spectrum of the garnet represented in the lower part of the diagram in Figure 14b.

The high field strength Nb and Ta pair, with equal charge and very similar ionic radii, are highly incompatible, which is probably related to the tendency shown by garnets from evolved pegmatites to be enriched in these elements (Figure 13a). However, some garnet crystals from the Berry-Havey pegmatite show a marked internal zoning from core to rim with a gradual decrease in the Nb and Ta content (Figure 15b). The occurrence of some large crystals of Nb-Ta oxides in the core margin of this pegmatite, close to the garnet layer, could be implied in the progressive decrease in Nb-Ta observed in these garnets as they crystallize. Another pair of trace elements that has often been used as a petrogenetic indicator in fractionated igneous environments is that of Zr and Hf. These elements are highly influenced by the presence of zircon, which may incorporate both elements in its structure. In the studied garnets certain differences are observed for the Zr and Hf content between fractionated and barren pegmatites, but there is not a clear discrimination, suggesting that the effect of minerals such as zircon is greater than that of the fractionation degree of the pegmatite. Other elements such as U and Th may be greatly affected by microinclusions of minerals such as zircon, xenotime-Y, and monazite-Ce. These microinclusions, common to all fractionated pegmatites in the Oxford field, may lead to irregular or non-existent zonation patterns in garnets for these elements (Figure 15).

Degassing of the melts at the fluid-magmatic stage during the formation of pockets in the core zone of pegmatites could also affect the trace elements contents in garnets. The petrographic features described for the garnet layer, including tourmaline rims around some garnet crystals, the partial dissolution of garnets, and the occurrence of microinclusions of some evolved species such as pollucite, suggest that garnet crystallization could be multistage: primary from the melt, and fluid-magmatic from an exsolved fluid coexisting with the melt (autometasomatic). At this stage, a redistribution of trace elements between melt-fluid-minerals or between crystals and fluid could happen.

6.2. Garnet as Indicator of Pegmatitic Fractionation

According to [52] garnets that crystallize from a highly evolved magma usually belong to the alm-sps solid solution and are relatively rich in Mn. In addition, garnets from pegmatites with a low fractionation degree are usually Fe-rich [1]. The results plotted in Figure 9a support both statements. For the studied pegmatitic garnets, samples from the most fractionated pegmatites are enriched in the spessartine component. In contrast, those from the barren pegmatites are enriched in the almandine component, and garnets from the intermediate Palermo No. 1 pegmatite show intermediate values, plotting between

both groups. Although less evidently, the corner of the diagram where the rest of the garnet species (Ca and Mg-rich) are represented, also reflects the fractionation degree of the hosting pegmatites. The barren bodies are the ones that contain the garnets with the highest Ca and Mg proportions, followed by Palermo No. 1 and, finally, garnets from the evolved pegmatites show almost negligible Ca and Mg content. This diagram may be useful for the pegmatite exploration, as the chemical compositions of garnets seem to reflect the magma evolution degree at the time of garnet crystallization.

The fractionation degree of pegmatites seems to be also reflected in the content of some trace elements in garnet. The clearest case is shown in Figure 13a, where Nb and Ta contents are higher for the more fractionated pegmatites and lower for the barren ones. The positive correlation between both elements shown by the garnets of the more fractionated pegmatites is nearly completely lost for garnets associated with barren pegmatites and migmatites. In garnet from Palermo No. 1, the positive correlation between Nb and Ta is maintained, although with a different slope from that of the samples from the most evolved pegmatites. These results have allowed establishing the three fields shown in Figure 13a, which could probably be used as a guide in the pegmatite exploration in the studied region.

Although less evident than the previous case, the Zr and Hf content of garnets (Figure 13b) may also serve to differentiate the most fractionated pegmatites, since they always present the highest values for both elements. In addition, garnets from the most evolved pegmatites tend to show contents farther from the CHARAC field than the rest (Figure 16).

Finally, the slopes of the HREE spectra of garnet (Figure 14) may constitute another geochemical indicator of the fractionation degree of pegmatites, since those from the barren pegmatites tend to show positive slopes; those from intermediate pegmatites show both positive and negative slopes; and garnets from the most fractionated bodies show flat or negative slopes (Figure 14).

Therefore, according to the results obtained in this work, some major and trace elements in garnets may potentially be used in order to discriminate between fractionated and barren pegmatites in the Oxford pegmatitic field. However, in order to determine if these geochemical indicators of garnet may be applicable to other pegmatitic belts in the world, it would be necessary to analyze a greater number of pegmatitic garnets from other locations and from different zones within those pegmatites. That way, it could be corroborated if the trends observed in this study are maintained and, if so, it could be possible to establish more precisely the compositional limits for the three suggested fields: i.e., evolved, intermediate, and barren pegmatites. In addition, and taking into account the different models for the generation of pegmatitic melts (mainly anatectic versus magmatic), it could be interesting to compare the trace elements contents of garnets from pegmatites with different origins, to check if these data may help in deciphering the origin of the pegmatitic melts.

7. Conclusions

The present work, carried out on garnet crystals from some of the Oxford field pegmatites and Palermo No. 1 pegmatite, allows us to reach the following conclusions:

1. All of the studied pegmatites contain garnets belonging to the almandine-spessartine series, the Mn-rich component becoming higher as the fractionation degree increases.
2. These garnets show increasing Mn and decreasing Fe contents from core to rim. The rest of the chemical elements analyzed show a variety of zoning patterns and cannot be related to the fractionation degree of the pegmatite.
3. Niobium and Ta show a clear positive correlation and the highest values for the most fractionated pegmatites; intermediate values for the intermediate pegmatite; and no correlation and the lowest values for the barren pegmatites.
4. Garnets from barren pegmatites present the lowest Zr and Hf contents and the closest values to the CHARAC field.

5. HREE slopes in garnets are positive in barren pegmatites, and negative or subhorizontal in fractionated pegmatites. Garnets from the intermediate pegmatite show both positive and negative slopes.
6. The most useful elements to discriminate between barren bodies and fractionated pegmatites are controlled by more or less complex cationic substitution mechanisms, and influenced by the starting composition of the pegmatitic magma, by the competing effects of other coexisting mineral phases, and/or by autometasomatism due to the action of exsolved fluids in the fluid-magmatic stage.
7. In the studied region, the contents of the major elements Fe, Mn (Mg, Ca) and of the trace elements Ta, Nb, Zr, Hf, and HREE, as well as the Zr/Hf, Y/Ho ratios in garnets are proposed as potential indicators of the fractionation degree of pegmatites. It would be necessary to expand the number of garnet samples analyzed to pegmatites from other regions in order to corroborate the usefulness of these garnet geochemical indicators on a more general scale.

References

1. Müller, A.; Kearsley, A.; Spratt, J.; Seltmann, R. Petrogenetic implications of magmatic garnet in granitic pegmatites from Southern Norway. *Can. Mineral.* **2012**, *50*. [CrossRef]
2. Li, B.; Ge, J.; Zhang, B. Diffusion in Garnet: A Review. *Acta Geochim.* **2018**, *37*, 19–31. [CrossRef]
3. Kogel, J.E.; Trivedi, N.C.; Barker, J.M.; Krukowski, S.T. *Industrial Minerals & Rocks: Commodities, Markets, and Uses*; SME: Tuttle, OK, USA, 2006.
4. Grew, E.S.; Locock, A.J.; Mills, S.J.; Galuskina, I.O.; Galuskin, E.V.; Hålenius, U. Nomenclature of the garnet supergroup. *Am. Mineral.* **2013**, *98*, 785–811. [CrossRef]
5. Bastin, E.S. *Geology of the Pegmatites and Associated Rocks of Maine: Including Feldspar, Quartz, Mica and Gem Deposits*; US Government Printing Office: Washington, DC, USA, 1911.
6. Felch, M.; Falster, A.U.; Simmons, W.B. Iron-bearing pollucite and tourmaline replacement of garnet in the garnet line in the Mt. Mica and Havey Pegmatites, Western Maine. *Can. Mineral.* **2016**, *54*, 1071–1086. [CrossRef]
7. Simmons, W.B.; Laurs, B.; Falster, A.; Koivula, J.I.; Webber, K. Mt. Mica: A Renaissance in Maine's gem tourmaline production. *Gems Gemol.* **2005**, *41*, 150–163. [CrossRef]
8. Marchal, K.; Simmons, W.; Falster, A.; Webber, K. Geochemistry, mineralogy, and evolution of Li-Al micas and feldspars from the Mount Mica Pegmatite, Maine, USA. *Can. Mineral.* **2014**, *52*, 221–233. [CrossRef]
9. Roda-Robles, E.; Simmons, W.; Pesquera, A.; Gil-Crespo, P.P.; Nizamoff, J.; Torres-Ruiz, J. Tourmaline as a Petrogenetic monitor of the origin and evolution of the Berry-Havey pegmatite (Maine, U.S.A.). *Am. Mineral.* **2015**, *100*, 95–109. [CrossRef]

10. Felch, M. The Garnet Line in Oxford County, Maine Pegmatites. Ph.D. Thesis, University of New Orleans, New Orleans, LA, USA, 2014.

11. Moretz, L.; Heimann, A.; Bitner, J.; Wise, M.; Rodrigues Soares, D.; Ferreira Mousinho, A. The composition of garnet as indicator of rare metal (Li) mineralization in granite pegmatites. In Proceedings of the PEG 2013: The 6th International Symposium on Granitic Pegmatites, Barlett, NH, USA, 26 May–2 June 2013; p. 75.

12. Baldwin, J.R.; von Knorring, O. Compositional range of Mn-garnet in zoned granitic pegmatites. *Can. Mineral.* **1983**, *21*, 683–688.

13. Bitner, J.; Heimann, A.; Wise, M.; Soares, D.R.; Ferreira, A.C.M. Garnet and gahnite from the Borborema pegmatite province, Northeastern Brazil, as indicators of pegmatite evolution and potential for rare-metal mineralization. In Proceedings of the GSA Annual Meeting, Minneapolis, MN, USA, 9–12 October 2011; Geological Society of America: Minneapolis, MN, USA, 2011; Volume 43, p. 413.

14. Mitchell, N.J. The Composition of Garnet in Granitic Pegmatites as a Proxy for Melt Evolution and Rare Metal Potential. Master's Thesis, East Carolina University, East Carolina, NC, USA, 2017.

15. Rahmani Javanmard, S.; Tahmasbi, Z.; Ding, X.; Ahmadi Khalaji, A.; Hetherington, C.J. Geochemistry of garnet in pegmatites from the Boroujerd intrusive complex, Sanandaj-Sirjan zone, western Iran: Implications for the origin of pegmatite melts. *Mineral. Petrol.* **2018**, *112*, 837–856. [CrossRef]

16. Samadi, R.; Miller, N.R.; Mirnejad, H.; Harris, C.; Kawabata, H.; Shirdashtzadeh, N. Origin of garnet in aplite and pegmatite from Khajeh Morad in northeastern Iran: A major, trace element, and oxygen isotope approach. *Lithos* **2014**, *208–209*, 378–392. [CrossRef]

17. Sokolov, Y.M.; Khlestov, V.V. Garnets as indicators of the physicochemical conditions of pegmatite formation. *Int. Geol. Rev.* **1990**, *32*, 1095–1107. [CrossRef]

18. Reusch, D.; Staal, C. The Dog Bay—Liberty line and its significance for Silurian tectonics of the northern Appalachian orogen. *Can. J. Earth Sci.* **2011**, *49*, 239–258. [CrossRef]

19. Tomascak, P.B.; Brown, M.; Solar, G.S.; Becker, H.J.; Centorbi, T.L.; Tian, J. Source contributions to Devonian granite magmatism near the Laurentian border, New Hampshire and Western Maine, USA. *Lithos* **2005**, *80*, 75–99. [CrossRef]

20. Wise, M.A.; Brown, C.D. Mineral Chemistry, petrology and geochemistry of the Sebago granite-pegmatite system, Southern Maine, USA. *J. Geosci.* **2010**, *55*, 3–26. [CrossRef]

21. Brown, M.; Solar, G.S. Granite ascent and emplacement during contractional deformation in convergent orogens. *J. Struct. Geol.* **1998**, *20*, 1365–1393. [CrossRef]

22. Solar, G.S.; Brown, M. Petrogenesis of migmatites in Maine, USA: Possible source of peraluminous leucogranite in Plutons? *J. Petrol.* **2001**, *42*, 789–823. [CrossRef]

23. Guidotti, C.V. Metamorphism in Maine: An overview. *Stud. Maine Geol.* **1989**, *3*, 1–19.

24. Holtz, F.; Behrens, H.; Dingwell, D.B.; Johannes, W. H_2O solubility in haplogranitic melts: Compositional, pressure, and temperature dependence. *Am. Mineral.* **1995**, *80*, 94–108. [CrossRef]

25. Solar, G.; Tomascak, P. *The Migmatite-Granite Complex of Southern Maine: Its Structure, Petrology, Geochemistry, Geochronology, and Relation to the Sebago Pluton*; Maine Geological Survey Publication: Reston, VA, USA, 2016.

26. Simmons, W.; Falster, A.; Webber, K.; Felch, M.; Bradley, D.; Roda-Robles, E.; Freeman, G.; Morrison, J.; Nizamoff, J. Lithium-Boron-Beryllium gem pegmatites, Oxford Co., Maine: Havey and Mount Mica Pegmatites. In Proceedings of the 2017 New England Intercollegiate Geological Conference, Bethel, ME, USA, 29 September–1 October 2017.

27. Bradley, D.; Shea, E.; Buchwaldt, R.; Bowring, S.; Benowitz, J.; O'Sullivan, P.; McCauley, A. Geochronology and tectonic context of Lithium-Cesium-Tantalum pegmatites in the Appalachians. *Can. Mineral.* **2016**, *54*, 945–969. [CrossRef]

28. Wise, M.A.; Francis, C.A. Distribution, classification, and geological setting of granitic pegmatites in Maine. *Northeast. Geol.* **1992**, *14*, 82–93.

29. Simmons, W.; Falster, A.; Webber, K.; Roda-Robles, E.; Boudreaux, A.; Grassi, L.; Freeman, G. Bulk composition of Mt. Mica pegmatite, Maine, USA: Implications for the origin of an Lct type pegmatite by anatexis. *Can. Mineral.* **2016**, *54*, 1053–1070. [CrossRef]

30. Webber, K.L.; Simmons, W.B.; Falster, A.U.; Hanson, S.L. Anatectic pegmatites of the Oxford County pegmatite field, Maine, USA. *Can. Miner.* **2019**, *57*, 811–815. [CrossRef]

31. Osberg, P.; Hussey, A.; Boone, G. *Bedrock Geologic Map of Maine*; Maine Geological Survey Maps: Massachusetts, NH, USA, 1985.

32. Nicholson, S.W.; Dicken, C.L.; Horton, J.D.; Foose, M.P.; Mueller, J.A.L.; Hon, R. *Preliminary Integrated Geologic Map Databases for the United States: Connecticut, Maine, Massachusetts, New Hampshire, New Jersey, Rhode Island and Vermont*; Open-File Report; U.S. Geological Survey: Washington, DC, USA, 2006; Volume 2006–1272, p. 49.

33. Roda-Robles, E.; Simmons, W.; Pesquera, A.; Gil-Crespo, P.P.; Torres-Ruiz, J. Estudio de los granates asociados a la pegmatita de elementos raros Berry-Havey (Maine, EEUU): Variaciones composicionales e implicaciones petrogenéticas. *Rev. Soc. Esp. Mineral.* **2014**, *19*, 1–2.

34. Pouchou, J.L.; Pichoir, F. *"PAP" φ(PZ) Procedure for Improved Quantitative Microanalysis: Microbeam Analysis*; San Francisco Press: San Francisco, CA, USA, 1985; pp. 104–106.

35. Simmons, W.B.; Falster, A.U.; Webber, K.L.; Roda-Robles, E. Mount Mica Pegmatite, Maine, USA. In *PEG2013: The 6th International Symposium on Granitic Pegmatites, Fieldtrip Guidebook*; Rubellite Press: New Orleans, LA, USA, 2013; pp. 135–136.

36. Falster, A.U.; Nizamoff, J.W.; Simmons, W.B.; Whitmore, R.W.; Roda-Robles, E.; Sprague, R.A.; Freeman, G. The Palermo Phosphate-Rich Pegmatite, New Hampshire. In *Fieldtrip Guidebook*; Rubellite Press: New Orleans, LA, USA, 2013.

37. Whitney, D.; Evans, B. Abbreviations for names of rock-forming minerals. *Am. Mineral.* **2010**, *95*, 185–187. [CrossRef]

38. Falster, A.U.; Simmons, W.B.; Webber, K.L.; Dallaire, D.A.; Nizamoff, J.W.; Sprague, R.A. The Emmons Pegmatite, Greenwood, Oxford County, Maine. *Rocks Miner.* **2019**, *94*, 498–519. [CrossRef]

39. Černý, P.; Ercit, T.S. The classification of granitic pegmatites revisited. *Can. Mineral.* **2005**, *43*, 2005–2026. [CrossRef]

40. Nizamoff, J.W.; Whitmore, R.W. *The Palermo Pegmatites, North Groton, New Hampshire*; Rubellite Press: New Orleans, LA, USA, 2013.

41. McDonough, W.F.; Sun, S.-S. The composition of the Earth. *Chem. Geol.* **1995**, *120*, 223–253. [CrossRef]

42. Cerny, P.; Meintzer, R.E.; Anderson, A.J. Extreme fractionation in rare-element granitic pegmatites; Selected Examples of Data and Mechanisms. *Can. Mineral.* **1985**, *23*, 381–421.

43. Chernoff, C.B.; Carlson, W.D. Disequilibrium for Ca during growth of pelitic garnet. *J. Metamorph. Geol.* **1997**, *15*, 421–438. [CrossRef]

44. Černỳ, P. Exploration strategy and methods for pegmatite deposits of tantalum. In *Lanthanides, Tantalum and Niobium*; Springer: Berlin/Heidelberg, Germany, 1989; pp. 274–302.

45. London, D. Pegmatites: The Canadian mineralogist special publication 10. *Mineral. Assoc. Can. Que. Can.* **2008**, 347. [CrossRef]

46. Roda-Robles, E.; Galliski, M.; Roquet, B.; Hatert, F.; Paeseval, P. Phosphate nodules containing two distinct assemblages in the cema granitic pegmatite, San Luis Province, Argentina: Paragenesis, composition and significance. *Can. Mineral.* **2012**, *50*, 913–931. [CrossRef]

47. García-Serrano, J. Distribución del Fe-Mn-(Mg) en Silicatos y Fosfatos Primarios de La Pegmatita Emmons (Maine, EEUU), e Implicaciones para su Evolución Interna. Master's Thesis, University of Granada, Granada, Spain, 2016.

48. Allan, B.D.; Clarke, D.B. Occurrence and origin of garnets in the South Mountain Batholith, Nova Scotia. *Can. Mineral.* **1981**, *19*, 19–24.

49. Bau, M. Controls on the fractionation of isovalent trace elements in magmatic and aqueous systems: Evidence from Y/Ho, Zr/Hf, and lanthanide tetrad effect. *Contrib. Mineral. Petrol.* **1996**, *123*, 323–333. [CrossRef]

50. Breiter, K.; Novák, M.; Koller, F.; Cempírek, J. Phosphorus–An omnipresent minor element in garnet of diverse textural types from leucocratic granitic rocks. *Mineral. Petrol.* **2005**, *85*, 205–221. [CrossRef]

51. Roda-Robles, E.; Pesquera, A.; Simmons, W.; Gil-Crespo, P.P.; Webber, K.; Nizamoff, J.; Falster, A. Paragenetic relationships, geochemistry and petrogenetic significance of primary Fesbnd Mn phosphates from pegmatites: The case study of Cañada (Salamanca, Spain) and Palermo (New Hampshire, USA) pegmatites. *Lithos* **2020**, *374*, 105710. [CrossRef]

52. Manning, D.A.C. Chemical variation in Garnets from aplites and pegmatites, peninsular Thailand. *Mineral. Mag.* **1983**, *47*, 353–358. [CrossRef]